BRNO UNIVERSITY OF TECHNOLOGY
VYSOKÉ UČENÍ TECHNICKÉ V BRNĚ

FACULTY OF MECHANICAL ENGINEERING
FAKULTA STROJNÍHO INŽENÝRSTVÍ

HEAT TRANSFER AND FLUID FLOW LABORATORY
LABORATOŘ PŘENOSU TEPLA A PROUDĚNÍ

LOW-COST FILTRATION BARRIERS FOR ULTRAFINE PARTICLES SEPARATION

LEVNÉ FILTRAČNÍ PŘEPÁŽKY PRO SEPARACI ULTRAJEMNÝCH ČÁSTIC

DOCTORAL THESIS – SHORT VERSION
TEZE DIZERTAČNÍ PRÁCE

AUTHOR — Ing. Pavel Kejík
AUTOR PRÁCE

SUPERVISOR — prof. Ing. Tomáš Svěrák, CSc.
ŠKOLITEL

BRNO 2019

KEYWORDS

Alkali activation, alkali-activated materials, geopolymer, blast furnace slag, fly ash, filtration, separation

KLÍČOVÁ SLOVA

Alkalická aktivace, alkalicky aktivované materiály, vysokopecní struska, elektrárenský popílek, filtrace, separace

CONTENT

1 STATE OF ART

The main AAMs that are of growing interest in recent years are metakaolin-based geopolymers and subsequently the most research (and papers published) relates to geopolymers thus the technology, including the porous structures and even tailoring the porosity (Landi et al, 2013), is more advanced than in the case of other AAMs on the basis of secondary raw materials such as FA and BFS. This section therefore combines the results form papers dedicated to secondary raw materials based AAMs with relevant studies of the conventional geopolymers.

The first contemporary published attempts on similar aluminosilicate filtering media on the basis of industrial secondary raw materials come from 1990's, e.g. Jo et al (1996). These filters were however prepared by sintering and this line of research still continues parallel to the alkali-activation of these materials with very promising results (Jedidi et al, 2011; Tewari et al, 2010; Qin et al, 2015; Cao et al., 2014; Fang et al, 2013; Singh et Bularasa, 2013). However, if there is a way to achieve comparable results only by chemical reaction, a big amount of energy would be saved, which is the reason why studies like this dissertation are important.

Another direction of research directly in the field of alkali activated porous materials is their foaming mainly by adding silica fumes containing free silicon which is oxidized by water in the mixture releasing hydrogen (Prud'homme et al, 2010; 2011A; 2011B). However, the foams had not defined pore size because the bubbles tend to join together (which is not in most authors' main aim because the purpose of the studies is the material's light weight and favorable thermal insulation properties for future utilization in building industry). Recently, however, Zhang et al (2016) published a paper on controlling the foam porosity via two-step phase-conversion technique comprised of geopolymer foaming and hydrothermal crystallization. Previously, Henon et al. (2012) published a paper on possibility of controlling the porosity using various temperature cycles that also decreased the time of synthesis.

Medpelli et al (2014) introduced a very interesting technique for porous geopolymer preparation by mixing triglyceride oil into a freshly made geopolymer paste to form a reactive emulsion. During the curing process, the oil in the alkaline emulsion undergoes a saponification reaction to be decomposed to a water-soluble soap and glycerol molecules which are then extracted from the cured material simply using hot water.

The general history of alkali activation was further described above. The utilization of alkali-activated materials in preparation of filtration media has been of interest for only a decade or so if we do not take into account the alumino-silicate materials for immobilization of dangerous substances containing heavy metals by adsorption which has been researched since 1990s (Van Jaarsveld et al., 1997) and contain very interesting applications, for example Pb and Cu immobilization by FA-based AAM (Phair et al, 2004), removal of sulphates over barium-modified BFS AAM (Runtti et al, 2016), removal of cesium from aqueous solution by adsorption on mesoporous FA/BFS AAM (Lee et al, 2017), etc. Wang et al (2006) conducted work describing alkali-activation FA conversion into effective adsorbent for removal of heavy metals and dyes from wastewater. The true filtration separation techniques utilizing geopolymers/AAMs are e.g. gas oil in water emulsion separation on Taguchi method-synthesized BFS membrane (Mohammadi et Mohammadi, 2017), separation of water from ethanol on alkali activated BFS membrane (Azarshab et al, 2016).

Very interesting is the way of production and also the application of porous AAM prepared by Duan et al (2016). Porous material on the basis of FA was partially (30%wt.) replaced by iron ore tailings, H_2O_2 was added as a foaming agent, the mixture was activated by alkaline silicate solution and the material was tested (successfully) for spontaneous adsorption of Cu^{2+} from wastewater.

One of the first papers to address, among other things, directly the porosity of alkali-activated materials was published by Duxson et al. (2005) and it is named "*Undestanding the relationship between geopolymer composition, microstructure and mechanical properties"*. This paper inspired author of this work to study the porosity of the material directly through the ratio of the main oxides because the work shows the differences in structure based simply on the Si:Al ratio change.

There are not many articles on combination of fly ash and slag during alkali activation but there is a particularly important one recently published by Ye et Radlińska (2016) summarizing some of the key information about the microstructure formation.

A very good review on the topic of alkali-treatment recycling of fly ash and pozzolanic industrial by-products was recently published by Lee at al. (2017B). A zeolite framework synthesis and methods of appropriate research are presented in the paper. It also includes a chapter of fly ash acid pretreatment to remove CaO and Fe_2O_3 'impurities'.

Note: The fact was known when designing this works procedure but the pretreatment was not involved due to its complexity and energy- (and consequently cost-) demands especially for drying after the procedure as the intention of the work was to focus on the porous media preparation with the lowest theoretical cost possible. The level of CaO was however taken into account during the selection of the FA and the one with the lowest content was chosen for the experiments.

Another method of fly ash pretreatment, namely mechanical activation, was studied by Temuujin et al (2009) and Chindaprasirt et Rattanasak (2010) both concluding that the mechanical activation improves the compressive strength of the resulting AAM material to 40MPa on average.

Note: Mechanical activation was studied experimentally in this work and the strength results seem to be convincing. It was however not involved into the experimental procedure because of the fineness of the material - fly ash has very fine granulometry even in unaffected state and the classification has to be done to get rid of the finest portions (which embody a significant part of the bulk) to obtain fractions that can be used to prepare defined porous material via 'dry' press-molding of defined particle fractions. After series of grinding experiments on stirred media mill and then air jet mill in various regimes it was concluded that the processing was either not effective enough to substantially support the activity of the material or in other cases it meant an increase in the finest portions (that are not applicable for the porous material production) in a scale that do not justify the demand for energy spent on comminution and classification procedures neither the amount of extra material becoming useless for the work after this pretreatment.

Every year more and more authors study the factors affecting the mechanical properties, microstructure and composition of alkali-activated materials on the basis of secondary raw materials (e.g. relatively detailed study on red mud and FA gepolymers by Zhang et al., 2014).

A study conducted by Görkhan et Görkhan (2014) researched the influence of NaOH concentration on the mechanical properties of FA based AAM mortar cured at different temperatures and different curing times. They concluded that the increase in the curing time and the activator concentration affects the compressive strength as well as the porosity and consequently bulk density.

AAMs based on FA were also studied from the technological point of view by Nematollahi et Sanjayan (2014). The research was on use and effectivity of different commercial superplasticizers to increase workability of alkali-activated fly ash pastes.

Another recent study by Nedeljković et al (2018) investigates natural carbonation of AAS and FA pastes after one year and its influence on elastic modulus and porosity. The study concludes the fact that increasing BFS content decreases the occurrence of carbonation, so it is mainly an issue of FA-based AAMs.

On the other hand purely BFS-based AAMs have a different technological issue which is their shrinkage. Ye et Radlińska (2017) did the research of the polymerization shrinkage and came with a conclusion that the high-magnitude shrinkage in AAS is attributed to the high visco-elastic/visco-plastic pliability of calcium aluminosilicate hydrate (C-A-S-H) in the material and it can be considerably reduced via high-temperature curing. This would however unfortunately lead back to the energy-intensive treatment. Tthere are apparently better options concerning in particular shrinkage reducing admixtures (Bílek et al., 2016).

A study on how elevated temperatures (800°C) affect the geopolymers and geopolymer composites was done by Kong et Sanjayan (2008) and another related study comparing fire-resistance (800-1000°C) of fly ash AAM and ordinary Portland cement was conducted by Sarker et al. (2014). The first mentioned study favors geopolymer in front of geopolymer/aggregate composite, the second concludes that geopolymers hold their mechanical properties far better than Portland cement based specimens after the elevated temperature exposure. There is also a study from Mill-Brown et al. (2013) concluding that geopolymers reinforced with silicon carbide exhibit hold stable thermal properties up to 1000°C, tensile properties highlight a significant reduction in stiffness at up to 760°C however showing sufficient retention of ultimate tensile strength to suggest potential for use in high temperature applications. The last to mention at the point is a study by Nikliоć et al (2016) researching thermal stability of blended binders on the basis of FA and electric arc furnace slag which claim that the addition of slag improves the strength of FA-based AAMs, however it also negatively affects the thermal stability above 600°C.

Adsorption as an integral part of separation techniques was already mentioned above. Porous geopolymers/AAMs have been researched and utilized in the field for more than two decades as they are capable of removing heavy metals, but this way they can be utilized also as a catalysts. In the study published by Zhang et Liu (2013) geopolymer adsorbent (with 17-700 nm pores) was used as a catalyst for degradation of dye from wastewater.

The field that already utilizes the advantages of AAMs made on the basis of secondary raw materials is building industry where the conventional concrete based on Portland cement can be partially or fully replaced by geopolymer concrete which pervious and mechanical properties are very similar to its conventional substitute (Tho-In et al., 2012). Due to a review on cement

production conducted by Schneider et al. (2011) Holcim company produced in total of annual production only 4% of 'fly ash cement' and 8% of 'slag cement' in 1995 whereas in 2009 it was 26% of fly ash cement and 9% of slag cement (there is also a 'pozzolan cement' produced which between the years stays at 9%).

In the field of ordinary metakaolin-based geopolymers Zhang et al. (2014B) found out that substitution of 10% of metakalolin by FA increases the reaction extent, 28-day compressive strength by 15%, and also increases the porosity of the resulting material with increasing level of fly ash replacement.

A porosity-related patent on geopolymers was published in 2010 in US by Frizon et al. named *Method of preparing a controlled porosity geopolymer, the resulting geopolymer and the various application thereof*. It is metakaolin-based material but the technology when further developed should be usable within the secondary raw sources based geopolymers as well.

The last studies to mention study the porosity/permeability of alkali-activated materials from the opposite point of view – to lower it as much as possible. A study aiming to develop new sealant material for carbon capture and storage wells used for the process of geological sequestration of CO_2 (Nasvi et al., 2013 and 2014) came up with a geopolymer material that has maximum permeability of 0.04μD which is 5000 times lower than the permeability value recommended by the American petroleum industry (API) which makes this geopolymer material potential primary sealant in a typical wellbore. On top of that Haider et al (2013) also studying the suitable materials for geo-sequestration of CO_2, only in saline aquifers, found that geopolymer materials cured in saline water show higher strength results than the ones cured in normal water. This discovery is very promising because Portland cements based oil well cements have unfavorable properties when cured in saline water.

Note 1: *Due to Davidovits the term 'alkali-activated materials' should not be interchanged with 'geopolymers'. He postulates that geopolymers are only materials based on metakaolin (Al peak in position 55 in their NMR spectrum). The other related materials mostly based on other resources are called plainly AAMs. The background of their formation and their substantial composition are however the same in most aspects. The author uses both terms carefully due to his best knowledge and belief, but in some cases it can be confusing due to interchanging the terms in literature and the need to quote these sources correctly or simply because most of the processes valid for all AAMs were explained on geopolymers and the literature deals with them accordingly.*

Note2: *The "State of Art" chapter had to be reworked due to the fact that the most relevant articles and papers on this theme were published very recently because this field of study is of growing interest. Because of this fact it may contain new information not known and thus not taken to account when the experimental part of the work was designed and performed.*

2 EXPERIMENTAL PART

2.1 MATERIALS

The compositions of solid bulk materials used for the experimental work are listed in Table 1, 2 and 3 and Figure 1 shows their granulometries before and after classification. Table 4 contains compositions of liquid alkali activators, namely sodium hydroxide solution and water glass used to activate the mixtures for the testing bodies preparation.

Table 1: Prunéřov II fly ash oxide composition.

Main oxides (%wt.)									
SiO_2	Al_2O_3	CaO	Na_2O	K_2O	MgO	SO_3	Fe_2O_3	TiO_2	P_2O_5
47.3	23.2	6.0	0.6	1.6	1.2	2.3	15.5	1.3	0.2

Supplementary oxides (%wt.)									
Cr_2O_3	MnO	V_2O_5	NiO	CuO	ZnO	As_2O_3	Rb_2O	ZrO_2	SrO
0.04	0.15	0.06	0.02	0.02	0.04	0.02	0.02	0.03	0.05

BaO	CeO_2	Sm_2O_3	Tb_4O_7	Ho_2O_3
0.1	0.03	0.01	0.02	0.01

Table 2: Kotouč Štramberk slag oxide composition.

Oxides (%wt.)									
SiO_2	Al_2O_3	CaO	Na_2O	K_2O	MgO	SO_3	Fe_2O_3	TiO_2	MnO
34.7	9.1	41.1	0.4	0.9	10.5	1.4	0.3	1.0	0.6

Table 3: Bauxite oxide composition.

Composition (%wt.)			
Al_2O_3	Fe_2O_3	SiO_2	TiO_2
86.0	2.0	8.0	4.0

Table 4: Sodium hydroxide 50%wt. (left) and water glass (right) activators oxide compositions.

Composition (%wt.)	
Na_2O	H_2O
38.75	61.25

Composition (%wt.)		
Na_2O	SiO_2	H_2O
17.1	38.8	44.1

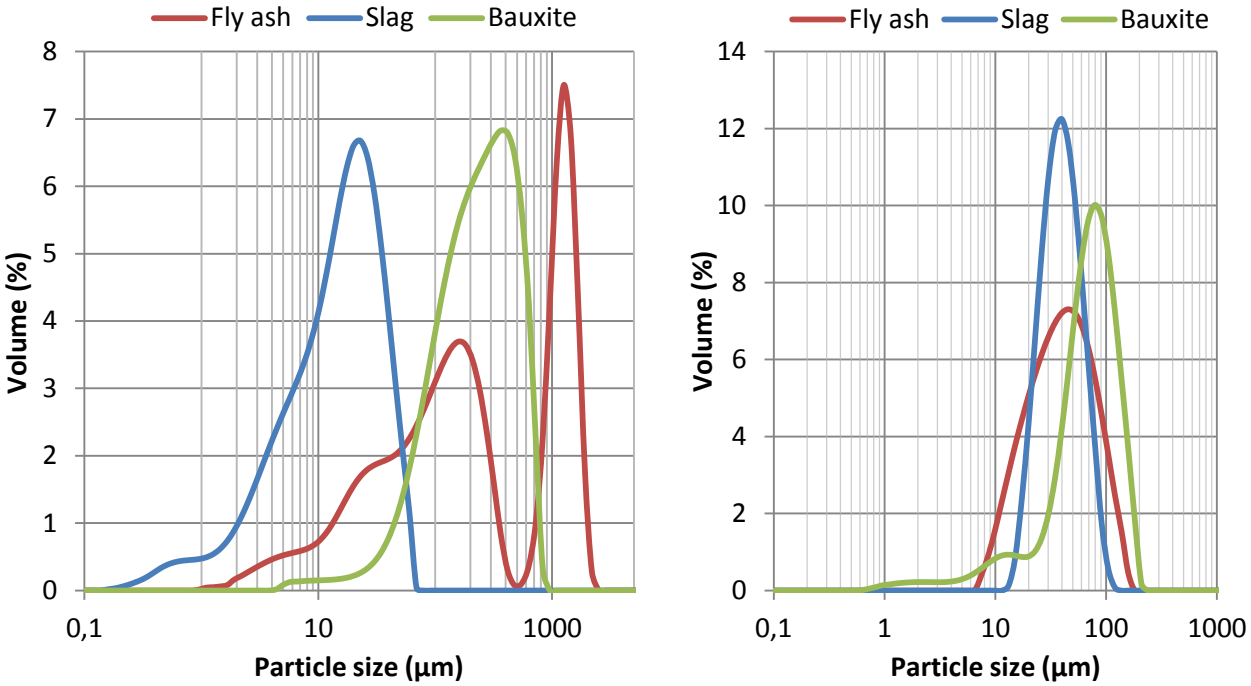

Figure 1: *Particular materials granulometries before and after classification.*

2.2 COMPOSITION CALCULATION PARAMETERS

Even after detailed exploration, it was not very clear what most of the experimental compositions listed in the literature are based on. Most authors state the parameters of the mixtures they tested but do not clarify why (Jedidi et al, 2011, Kim et al. 2013). To make this work more robust, it was necessary to make a solid basis. This had led the author to design a mathematical tool to calculate the mixture compositions based on basic variables used in preparation of ordinary geopolymers. This approach had never been used in this field.

After reviewing composition variables influencing the strength and stability of different alkali activated materials, three mentioned below were found to play a crucial role.

2.2.1 SiO_2:Al_2O_3

The first parameter of the geopolymer composition, often also reported as Si/Al ratio, determines the microstructure of the material. It simply originates from the alkali-aluminosilicate-hydrate (N-A-S-H) gel structure formation during the alkali activation of various aluminosilicates. The Si/Al ratio in N-A-S-H ranges generally approx. from 2.8 to 3.6. According to J. Davidovits 1991 work *Geopolymers: Inorganic Polymeric New Materials* activated materials are best formed with an Si:Al ratio in the range of 1 to 3. It has to be noted here that his work targeted the mechanical strength alone, not on the porosity development. Duxson et al in their later work from 2005 titled *Understanding the relationship between geopolymer composition, microstructure and mechanical properties* stated that the materials tend to be highly porous for Si/Al ratios ≤ 1.40 but largely homogenous for Si/Al ≥ 1.65. That means our first parameter in the oxide form SiO_2:Al_2O_3 (where there is one Si atom to two Al atoms) has to be in the range of 2.80 to 3.30 to obtain a desired porous structure.

2.2.2 $M_2O:Al_2O_3$

The second parameter was used for monitoring the charge balance in the bonding network. The activation process of aluminosilicate precursor initiates a polycondensation reaction leading to short-range ordered molecular network of SiO_4 and AlO_4 tetrahedrons joined by oxygen bridges. In this configuration, the AlO_4 tetrahedron introduces a negative charge, which the alkali metal balances by 'incorporation into the structure' or more precisely locating itself into the gaps between the tetrahedron structures (see chapter 2.5.3). Therefore it is clear that the ideal M:Al ratio is best to be a unity. Rowles and O'Connor concluded in their work *Chemical Optimisation of the Compressive Strength of Aluminosilicate Geopolymers Sythetized by Sodium Silicate Activation of Metakaolinite* in 2003 that compressive strength of the material maximizes when there is a slight excess of Na (M) beyond the unity, amounting up to 1.25. Their later work *Chemical and Structural Microanalysis of Aluminosilicate Geopolymers Sythetized by Sodium Silicate Activation of Metakaolinite* states that the charge balance of around unity is sufficient and a lot of excessive Na could even damage the emerging polymer network by terminating Si–O–Na chains and of course causing more efflorescence.

For the purpose of this work and its experimental task this variable was set down to 0.9–1.1 with experimental overlap up to 1.3 in some cases..

2.2.3 $H_2O:M_2O$

The third parameter was chosen to control the amount of water and this way the consistency and workability of the mixtures based on the work of Yusuf et al.: *Effects of H_2O/Na_2O molar ratio on the strength of alkaline activated ground blast furnace slag-ultrafine palm oil fuel ash based concrete, published in 2014*. Increase in this ratio negatively affects the final strength (Xie et Kayali,2016), but positively impact the mixture workability (Yusuf et al. 2014; Puertas et al. 2014). This parameter therefore does not have its optimum value set due to the chemical point of view but it is more intended for an optimization of the consistency for further processing.

For press-molding of the barriers, it was targeted to have the mixture as dry as possible, yet still capable of holding together after pressing because this way corresponds with the presumption that less water, in this case meaning more concentrated activator, increases the strength of the product (Singh et al, 2016; Kaur et al, 2018). The same conclusion comes out of the basic microscale conception that the best way to obtain the continuous microporous structure is to only wet the surface of the particles and to let the activator to dissolve the outer layer of the material and consequently create necks between them. It has to be mentioned though that this optimum consistency bound (dry part to liquid part ratio) is always applicable to certain particles granulometry and even their morphology and is obviously never sharp. On top of that the miscibility of the mixture even with the planetary-mixing machine is limited. The dryer the mixture the more difficult is to preserve good and even mixing in terms of necessary forces and related considerable heating – causing some part of already small amount of water to evaporate during the mixing process.

This variable had to be therefore empirically optimized from all perspectives mentioned above and is applicable only for used ingredients granulometry and even morphology as the rheology varies significantly with the particle shapes and is of greater importance the less of the fluid ingredient is in the system as it increases the interparticle hydrodynamic interactions.

This variable had to be later supplied or in some cases completely replace by simple water to solid ratio abbreviated in tables and text below as ‘w/s’ to correctly fulfill its role of consistency controlling parameter.

Note: *In this case focusing on low cost filtration materials sodium based alkali activators were used due to their price which is far much lower than the price of the second most common potassium-based ones. The true formulas of the 5.2.2 and 5.2.3 titles can be therefore written as* $Na_2O:Al_2O_3$ *and* $H_2O:Na_2O$ *but because the variables are valid for any alkali activator, the general formula was used in the titles.*

2.3 COMPOSITION CALCULATION METHODS

Two mathematical methods were designed for the computation of the geopolymer mixture compositions. The first and simpler method was programmed via the Solver in MS Excel, to verify the idea and test the results. The second more complex solution was developed and programmed afterwards using MATLAB.

Bauxite had to be added beyond the intended composition just to supply the aluminum oxide to the mixture and obtain suitable results following the set parameters. Otherwise it was not possible to achieve the ideal oxide ratios and the computation returned errors. There was given a condition of 10% maximal content of bauxite in the mixtures.

2.4 MIXTURES COMPOSITIONS

The MATLAB raw data containing over 70,000 results was gradually eliminated (mostly for near-duplicity or too high water content) and cropped but what remained was still slightly below half of the original dataset. Because the parameter P3 alone (as only an oxides ratio) did not sufficiently characterized the amount of water in terms of mixture consistency, water to solid ingredients ratio (equivalent to water/cement ‘w/c’ ratio in the concrete practice; labelled w/s in the tables and diagrams) had to be taken into account as well. During the subsequent searching 23 compositions were chosen that has the P1 and P2 values located across the whole intended ranges and at the same time differ in composition one from another. This way it was ensured that the following Table 5 sorted by any P parameter or any mixture component will cover the whole range of possible values of that particular parameter/component with certain distances although some of them in particular order may seem too close to each other. For example in the order below the table is sorted by fly ash content and it can be seen that the first two values are a bit too close, but the composition 1 and 2 have the ideal spacing in terms of sorting by blast furnace slag and also differ largely in P1 where they are located nearly on the opposite sides of the range. This way the required amount of mixtures was minimized yet any trend in results should be traceable and recognizable simply by sorting the results in the order corresponding to order of the desired parameter or component quantity.

Note: *The blue lines were added later as complementary values of parameters as close as possible to the lines with highlighted w/s which were still overly wet for the mold pressing and displaced liquids under the pressure. The line with red highlighted w/s does not have a suitable dryer substitute in the dataset.*

Table 5: MATLAB-based compositions chosen for experiments.

#	P1 (SiO_2/Al_2O_3)	P2 (Na_2O/Al_2O_3)	P3 (H_2O/Na_2O)	Glass	NaOH	Ash	Baux.	Slag	w/s
1	2.70	1.09	5.11	0.48	23.73	0.25	9.98	65.56	0.195
2	3.17	0.92	4.95	0.28	18.24	0.34	8.14	73.00	0.139
3	3.18	1.31	5.15	1.38	24.99	6.14	7.13	60.35	0.216
4	3.04	0.98	5.50	7.57	18.33	9.79	8.95	55.35	0.197
5	2.56	1.00	5.12	1.27	24.04	14.81	9.99	49.89	0.205
6	3.07	1.00	5.42	7.00	19.72	20.13	7.80	45.35	0.207
7	3.17	1.31	5.14	1.69	26.44	20.37	5.96	45.54	0.236
8	2.68	0.91	5.54	9.03	19.91	26.31	10.00	34.75	0.228
9	2.52	0.98	5.29	4.69	24.19	26.68	10.00	34.44	0.237
10	3.16	1.12	5.17	3.22	23.32	26.77	6.02	40.68	0.214
11	3.08	1.06	5.21	4.30	22.86	33.27	6.10	33.47	0.218
12	3.19	0.96	5.12	3.55	20.46	33.53	5.62	36.83	0.186
13	3.20	1.08	5.01	1.43	23.94	39.16	4.58	30.90	0.205
14	2.90	0.95	5.36	7.21	21.10	39.55	7.25	24.89	0225
15	2.35	0.90	5.15	2.94	25.79	44.54	9.96	16.77	0.240
16	3.10	0.90	5.62	11.95	17.81	45.38	6.49	18.36	0.230
17	3.16	1.05	5.09	3.16	23.86	48.72	4.24	20.02	0.219
18	3.18	1.07	4.98	1.30	25.48	56.54	3.12	13.57	0.221
19	2.99	0.90	5.31	7.57	21.01	59.05	5.34	7.04	0.227
20	2.76	0.95	5.12	3.67	24.99	59.65	6.01	5.68	0.237
21	2.44	0.90	5.01	1.23	27.06	60.64	7.89	3.18	0.239
22	2.79	0.90	5.05	3.13	24.17	63.95	5.52	3.24	0.223
23	3.20	0.93	4.83	0.61	23.72	73.24	1.84	0.60	0.196

Besides the mixtures obtained by MATLAB calculations also pure FA and BFS mixture series were prepared using only sodium hydroxide as an activator (see Table 12). Constitution of these mixtures was designed by empirical knowledge obtained until during the experimental work. The doses of activator were set to 6% and 12% of Na_2O with respect to the powder weight. The water to particulate w/s ratio, taking the NaOH inner water (NaOH ~ Na_2O + H_2O) into account, was 0.095 for 6% mixtures and 0.190 for 12% mixtures.

Table 6: Pure two-component fly ash (FA) and slag (S) mixtures compositions.

#	P1 (SiO_2/Al_2O_3)	P2 (Na_2O/Al_2O_3)	P3 (H_2O/Na_2O)	NaOH	Ash	Slag
FA-6	3.46	0.55	4.24	7.74	50	0
FA-12	3.46	0.92	4.73	15.48	50	0
S-6	6.47	1.26	4.67	7.74	0	50
S-12	6.47	2.35	5.02	15.48	0	50

The other question examined in connection with the previous one was the extent of activator concentration influence on the resulting strength of the AAM. It was examined due to observation

of increased friability of prepared FA-6 samples. For the purpose the calibration-like set of mixtures was designed with 1% to 6% dose of Na_2O. The water to particulate ratio was set to 0.095 for all the following mixtures (see Table 7).

Table 7: FA and S compositions for investigation of the activator concentration influences.

#	P1 (SiO_2/Al_2O_3)	P2 (Na_2O/Al_2O_3)	P3 (H_2O/Na_2O)	NaOH	Water	Ash	Slag
FA-1	3.46	0.19	12.15	1.29	3.96	50	0
FA-2	3.46	0.26	8.86	2.58	3.17	50	0
FA-3	3.46	0.33	6.97	3.87	2.38	50	0
FA-4	3.46	0.40	5.75	5.16	1.59	50	0
FA-5	3.46	0.47	4.89	6.45	0.80	50	0
FA-6	3.46	0.55	4.24	7.74	0	50	0
S-1	6.47	0.36	16.40	1.29	3.96	0	50
S-2	6.47	0.54	10.92	2.58	3.17	0	50
S-3	6.47	0.72	8.19	3.87	2.38	0	50
S-4	6.47	0.90	6.55	5.16	1.59	0	50
S-5	6.47	1.08	5.45	6.45	0.80	0	50
S-6	6.47	1.26	4.67	7.74	0	0	50

2.5 PREPARATION PROCEDURE

Due to very high viscosity of the mixture the mixing had to be done by planetary centrifugal mixer described above where the solid ingredients (already mixed together in ratio corresponding to the particular composition) were admixed by parts. The mixer was set to 2000 rpm for 3 times 20 seconds with manual mixing between runs. The time may appear too short but the 2000 rpm mix rapidly and first of all further mixing overheats the mixtures so they tend to compact and they also lose part of their workability due to loss of water by evaporation.

The mixture had to be then scattered manually and after weighting the intended amounts were transferred into molds already lined with support pad and flexible washer (described below). The mixtures had to be evenly spread across the mold before the pressing itself was executed to achieve the pressure as uniform over the area as possible. The pressing was performed at 1 ton for the barriers 25 mm in diameter which equals to approx. 1.99 kg/mm^2 ~ 19.5 MPa.

During the development of this method the flexible washers and pressing support pads were added to improve the mold emptying. The flexible washers made out of paper also helped in the removing process because the molding do not stick to the support pads and the washers themselves can be removed without damaging the product or in most cases peel off spontaneously by contortion under the effect of strong alkali on one side and dryer unaffected surface on the other.

After demolding the barriers were moist cured (closed in a tight box with wet sponge) under 70 °C for 24 hours. Due to research already done on the curing procedure of materials containing alkali activated materials 60-70 °C seem to be optimal temperature (Hardjito et al, 2009). Longer period of time (48h+) was concluded a bit better for the strength of the alkali activated materials, the difference in strength against the 24h cured materials was however not striking so it did not

justified the increased energy consumption. Therefore for the purpose of this work (trying to keep the consumption of production energy as low as possible) the shortest verified curing time was preferred (Memon et al, 2011; Bakharev, 2005; Van Jaarsveld et al, 2002; Rovnaník, 2010; Hardjito et al, 2004 and 2009).

Some of the bodies made of mixtures containing mostly GGBFS tended to bend or crack during the storage under laboratory conditions which is known phenomenon that happens due to considerable shrinkage of alkali activated slag-based materials (Bilim et Karahan, 2015; Bilim et al., 2013; Sakulich et Bentz, 2013). Therefore, the cured bodies were then stored in a box with increased humidity to maintain the moisture after the curing process which helped to eliminate the issue.

2.6 MECHANICAL TESTING

Geopolymers/AAMs are often mechanically tested by penetration tests. However mostly the materials are produced for utilization in construction applications so the hardness is of interest. Because this work deals with these materials as filtering media the product requirements are different and therefore the usual approach was abandoned and the bending strength testing was used instead. The strength of the materials was tested in four-point bending test on testing columns 10x10 mm in cross section. This test was preferred over the three-point bending because it is more appropriate for non-homogenous materials as it spreads the stress to a larger region of the testing body. Because there are no official standard testing methods for geopolymers/AAMs available the methodology used in this work is based on ČSN EN 12390-5 which is the Czech version of the European concrete testing standard EN 12390-5:2009 "*Testing hardened concrete. Flexural strength of test specimens"*.

Table 8: Uniaxial tensile strength measurements results in context with mixtures compositions and parameters, each result averaged from 4 measurements.

#	1	2	3	4	5	6	7	8	9	10	11	12	13	14	15	16	17	18	19	20	21	22	23
f_{ct} (Mpa)	4.8	6.9	7.3	7.0	4.9	5.6	3.5	4.3	5.3	6.2	4.9	7.7	6.3	5.7	3.7	6.2	6.0	6.6	6.5	4.4	2.5	5.5	5.6
St. Dev.	0.4	0.4	0.4	0.4	0.3	0.3	0.3	0.2	0.4	0.2	0.5	0.6	0.2	0.1	0.4	0.1	0.3	0.4	0.2	0.5	0.3	0.2	0.4

Table 8 shows all the MATLAB based mixtures' uniaxial tensile strength measurement results and their standard deviations altogether with the mixture parameters and compositions. Mixture 12 which is one of the driest (lowest w/s parameter) had achieved a maximal strength, namely 7.69 ± 0.57 MPa and mixture 21, which is the overall wettest one (highest w/s parameter), had the lowest overall strength of 2.53 ± 0.33 MPa. Composition number 3 that also exceeded 7 Mpa in uniaxial tensile strength testing has a majority of BFS in composition and contains more liquids than number 12The tensile strength on P1 dependence in Figure 2 confirms the premise that within the given range the strength of mixtures increases with increasing P1. Mixture 7 shows the biggest deviation from the main trend, but the P2 to *fct* dependence diagram offers an explanation in very

high P2 ratio where sodium can break down the polymer network by terminating Si–O–Na chains. This phenomenon is most likely influenced by water content because mixture 3 that has analogical values in all parameters but a different components ratio and much lower w/s ratio achieved very good strength. The lowest strength of the mixture 21 had to be caused by low P1 in combination with very high water content.

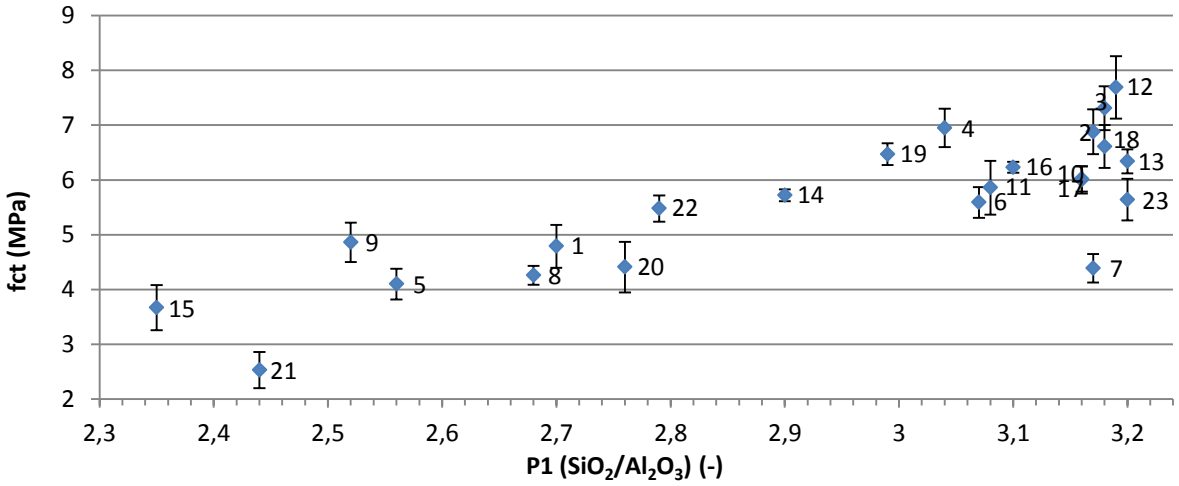

Figure 2: *Parameter P1 to uniaxial tensile strength dependence diagram.*

P2 to tensile strength dependence in Figure 3 does seem to show trend only in the lower bound of the cluster of values which tend to increase with P2.

In the diagram below (Figure 3) the strength is slightly decreasing with increasing w/s. The greatest deviation of mixtures 1 and 5 can be explained by their very low P1 (slightly over 2.5) that makes them less compact.

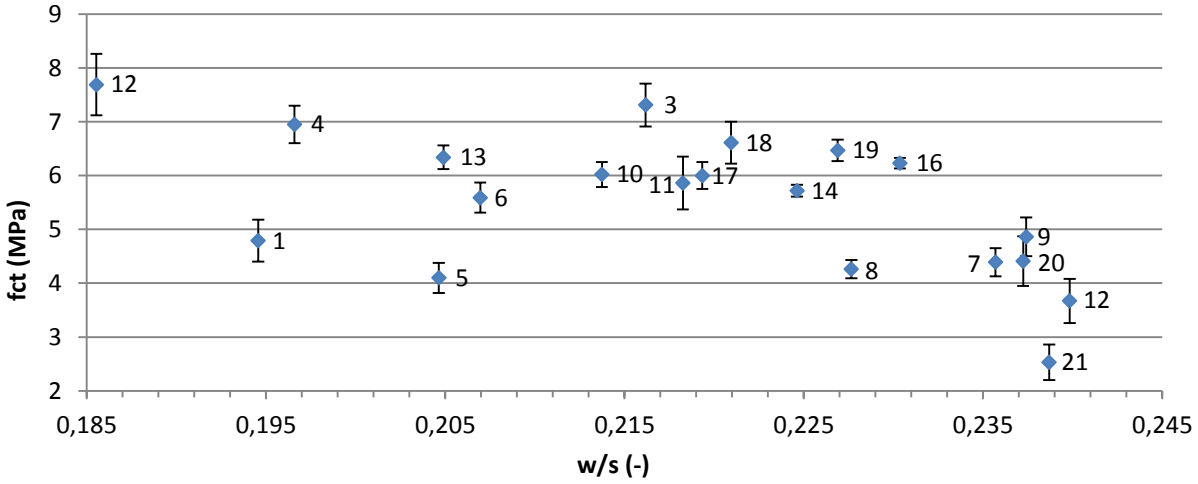

Figure 3: *Water to solid ratio to uniaxial tensile strength dependence diagram.*

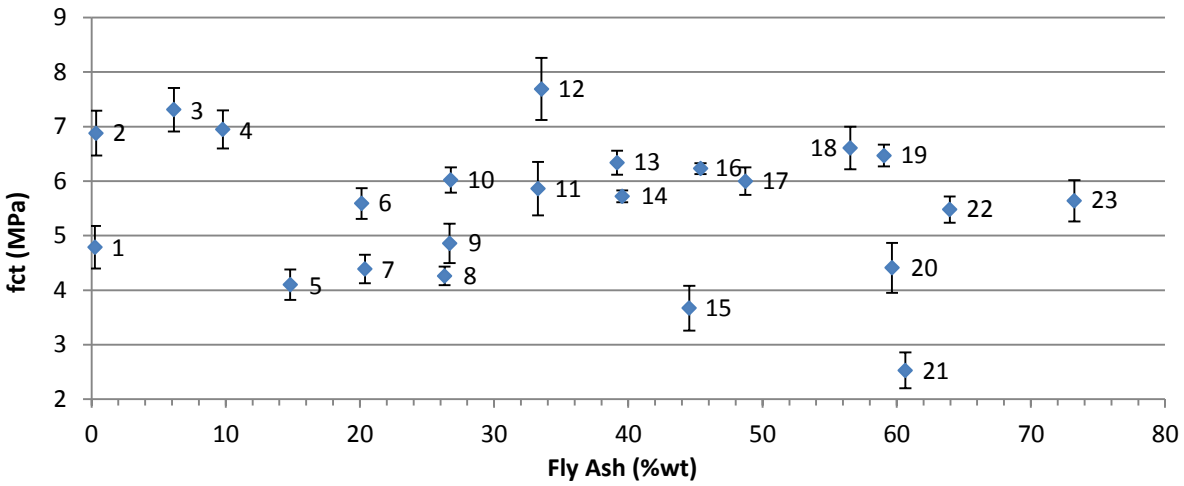

Figure 4: *Fly ash content to uniaxial tensile strength dependence diagram.*

Fly ash and slag content to tensile strength dependencies (Figure 4 and 5) do not show any trend whatsoever if we do not take into account that mixtures 15, 20 and 21 has the highest water content – after these are neglected it can be seen a slight tendency of the tensile strength to increase with increasing fly ash content and decrease with increasing slag content. However, this appearance does not match the tensile strength results of the two-component mixtures that are show in the Figure 6. Pure activated slag clearly achieved greater uniaxial tensile strengths in all mixtures of the testing series although for pure 50% NaOH utilization it greatly depends on the P2 value. In Table 9 parameter P2 increases to 0.92 for FA-12 and the strength increases in the same manner. For the slag series however, the strength maximum belongs to mixture S-5 which only slightly exceeds unity, but from there on it decreases as the Na_2O/Al_2O_3 ratio significantly increases.

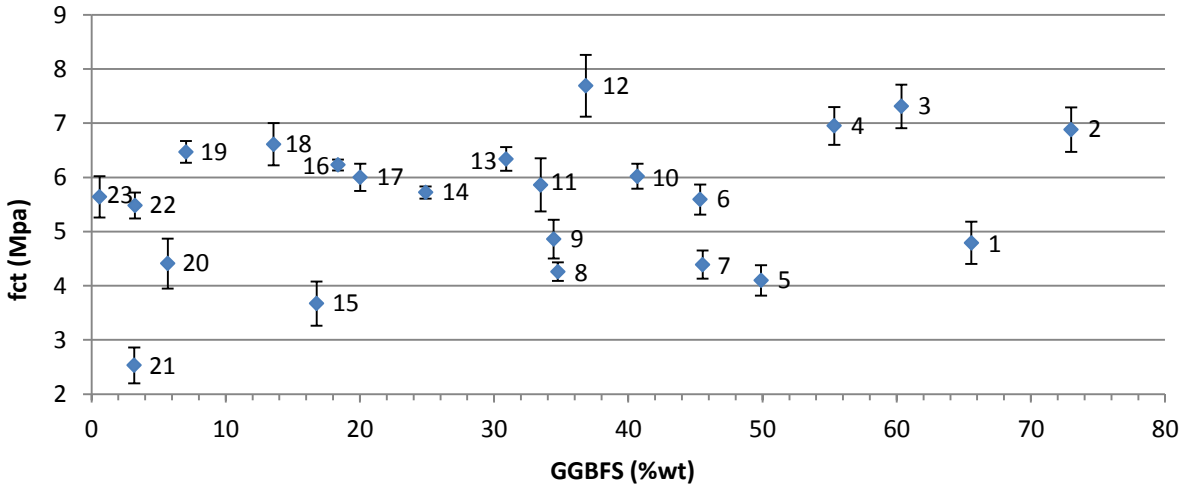

Figure 5: *Blast furnace slag content to uniaxial tensile strength dependence diagram.*

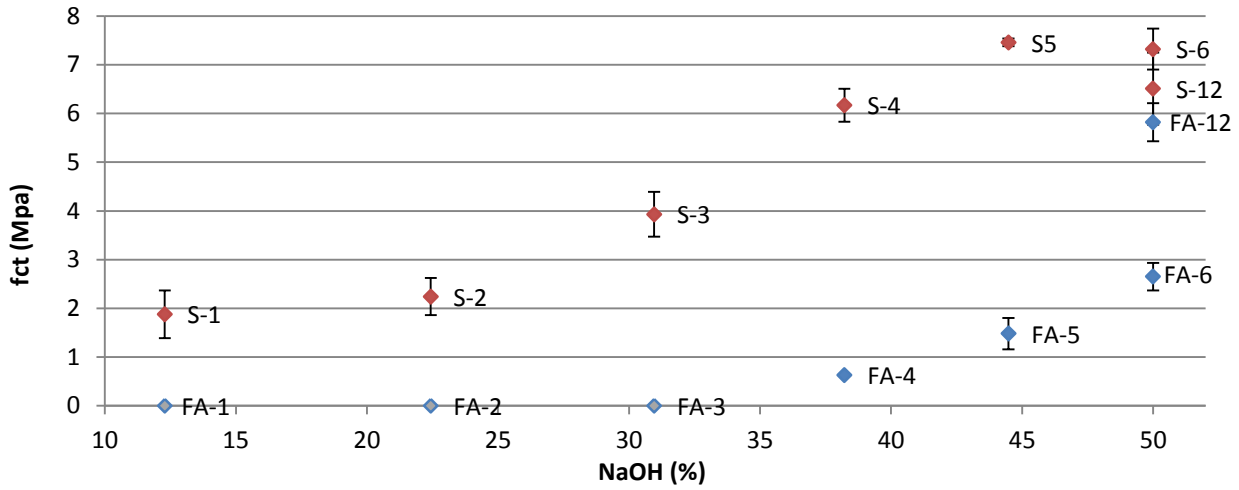

Figure 6: *Alkali activator (sodium hydroxide) concentration to uniaxial tensile strength dependence diagram of the fly ash and GGBFS based mixtures series.*

The FA-1, FA-2 and FA-3 mixtures in figure above were marked grey because they were not measured for uniaxial tensile strength as they could not be demolded without breakage.

In general it can be concluded that the strength parameters favor more GGBFS for the production of porous media. It is, however, questionable how much the particle morphology does influence the strength of the samples. GGBFS particles are angular compared to round shaped FA particles. If the GGBFS particles are in contact with each other along their edges or walls they have of course greater contact area although continuous porosity can be reduced.

Table 9: Uniaxial tensile strength results of the fly ash and GGBFS based mixtures in context with compositions and parameters, each result averaged from 4 measurements.

#	FA-1	FA-2	FA-3	FA-4	FA-5	FA-6	FA-12	S-1	S-2	S-3	S-4	S-5	S-6	S-12
Fct (MPa)	0.00	0.49	0.81	1.45	2.97	3.65	6.82	1.88	2.24	3.93	5.37	7.46	7.32	4.51
stand. deviation	0.00	0.17	0.35	0.56	0.32	0.28	0.39	0.49	0.38	0.46	0.34	0.08	0.42	0.54

2.7 POROSITY

The figures below show CFP (Capillary Flow Porosimetry) measurements with different ranges of pores contained in the filter barriers. The premise was that because the granulometry of the input ingredients is always the same, only in different ratios, the porosity results should depend greatly on the content of alkali activator that dissolves matter and then the resulting amount of forming N-A-S-H gel creates necks of various thicknesses between the particles. This assumption was to certain extent verified.

In the diagrams below (Figure 7) where only the relevant results are included can be seen that mixtures with mid to high content of water vary in pore size distributions in the range between approximately 0.07 to 0.65 µm but are not ordered by their water content. The lowest water content mixture which was number 2 had a through-pores sizes ranging from 0.7 to 6 µm. The second driest mixture which was number 12 however had pore sizes ranging from 0.3 to 0.8 µm and it shows greater pore content then most of the given series.

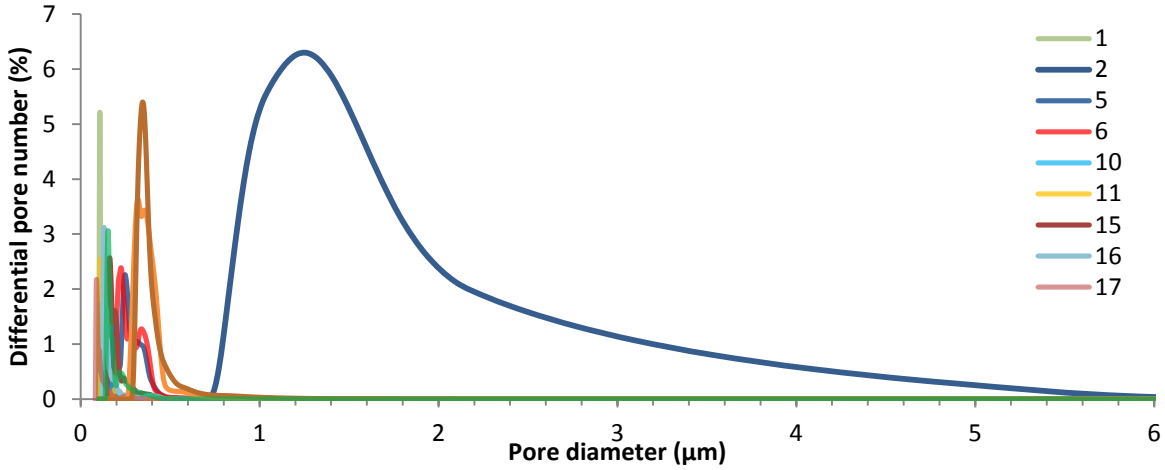

Figure 7: *CFP-based differential porosity curves of chosen MATLAB samples*

The next diagram (Figure 8) was cropped to show closely the range where most of the pore size distributions of the series are located and how its typical results look like. Nearly all the results (except sample 12) are located in this range but it is important to note that the reproducibility of the CFP measurements for more accurate specifications was not perfect due to manual production of the barriers. A lot of results also overlapped and the diagrams were then illegible. Therefore only the representative results were left to reveal the range of the pore diameters and the overall through-porosity of the samples that can be taken as certain for given feedstock granulometries and preparation conditions.

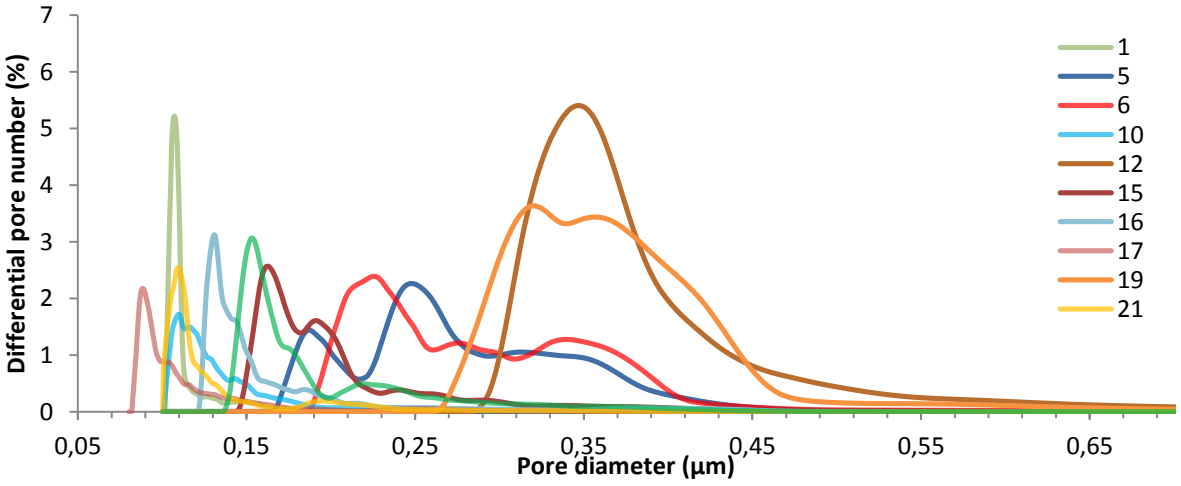

Figure 8: *CFP-based differential porosity curves of chosen MATLAB samples*

The FA and S series were also subjected to pore-distribution measurements via CFP and also MIP (Mercury Intrusion Porosimetry). The results are shown in Figures 9 to 16. It is important to note that both these techniques gave similar results regarding the observed trends when one significant peak occurs around certain pore diameter for every mixture composition, but the exact values of pore diameter differ significantly when compared the same mixture measurements by both methods. This is not surprising since the working principles of these methods are totally different and different is also evaluation of the results. While the CFP results are given in the percentual number of the pores of certain size with respect to the total amount of detected pores, the MIP results show volume changes of intruded mercury between the two different pore diameters normalized to the sample weight. It should also be noted that while MIP measures all opened pores including dead-end pores in the porous network, CFP is sensitive only to pores through which fluid can flow. CFP therefore better describes potential filtration properties. The MIP results were however converted to differential pore number form (Figures 11, 14 and 16) for better comparison.

Lower alkali-activator content specimens of the F (fly ash) series were very difficult to measure on the porosimetry due to their friability and fragility and therefore their results data were not included. However, the data left and compared in the diagrams below show that between the FA-6 and FA-12 both methods revealed larger pores present in specimens with lower activator dose (Figure 9). It is probably caused by lower N-A-S-H content creating narrower necks between particles as a consequence of lower solids dissolution. Pore size reduction at higher activator dose was also observed by increased intrusions of mercury into the pores smaller than 200 nm (Figure 10). Based on the total amount of intruded mercury and specimen volume, total porosity of FA-6 and FA-12 series was estimated to 38.5 ± 1.5% and 33.8 ± 2.9%, respectively. Despite the fact that the reproducibility was not ideal in some cases the results show very clearly that increased dose of activator lead to a decrease in total porosity.

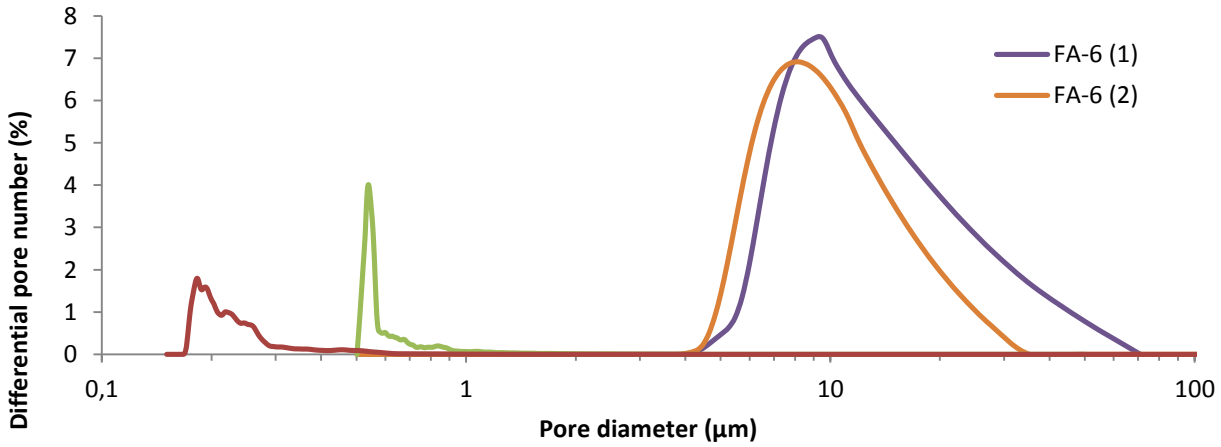

Figure 9: *CFP-based differential porosity curves of fly ash samples*

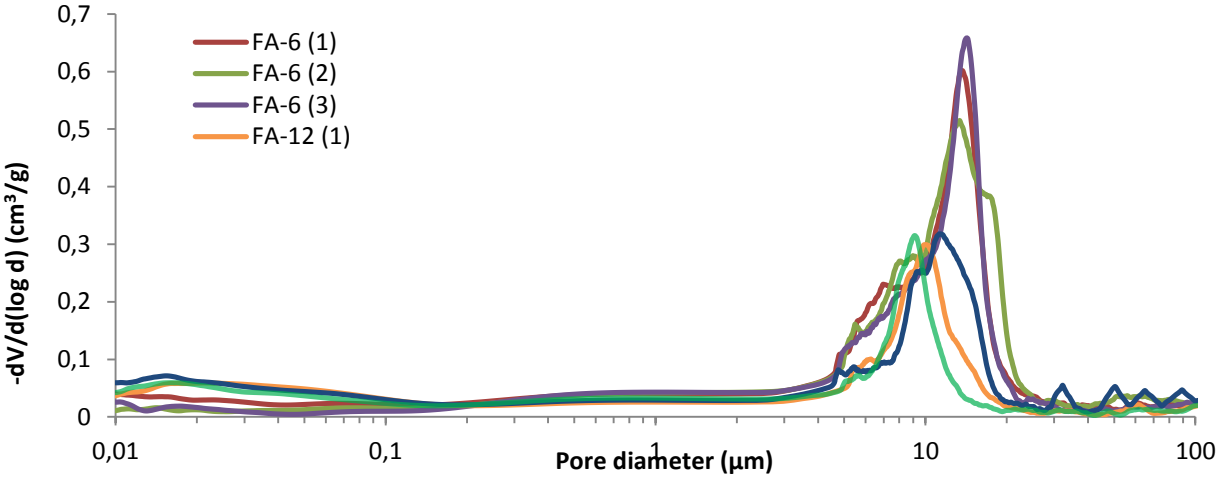

Figure 10: *MIP-based porosity measurements of fly ash samples expressed in volume change of intruded mercury into certain pore diameter normalized to the sample weight*

To compare the results among each other the MIP data was converted from their natural form of $-dV/d(\log d)$ (differential volume of intruded mercury normalized to one decade of pore-size channel related to the sample weight) to differential pore number dependence like the data from the CFP (see Figure 11). And it is now plain to see that the sample FA-12 (3) has its first peak around 1.3 µm even higher than all the FA-6 samples, which is not visible in the -d*V*/d(log *d*) form on the Figure 10.

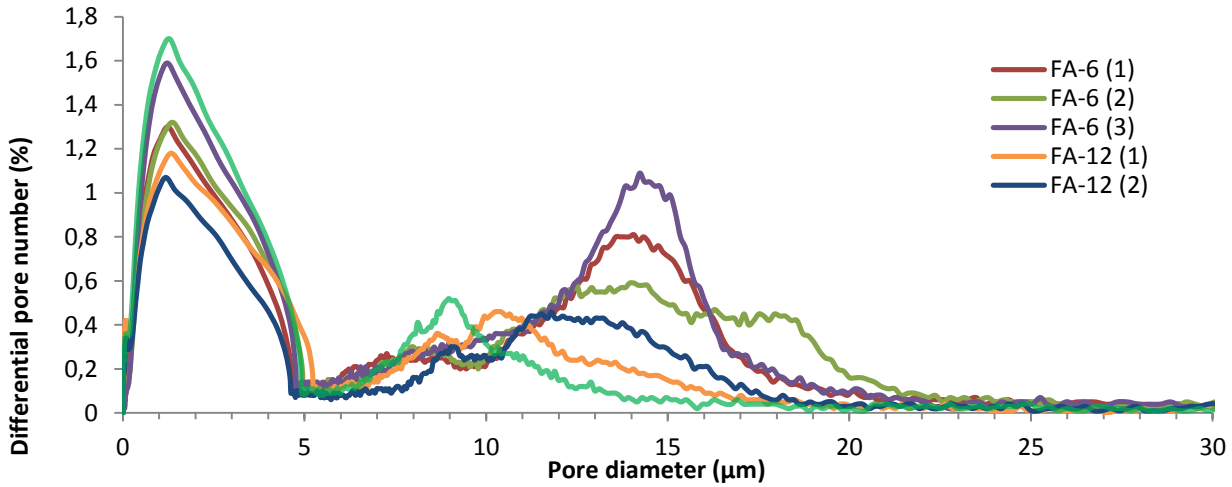

Figure 11: *MIP-based differential porosity measurements of fly ash samples*

The S (blast furnace slag) series of the samples that due to their higher overall strength (as discussed below) better withstand the porosimetry measurements even with lower dose of activator (except the lowest marked S-1) are shown in the following diagrams.

The CFP data clearly shows that the more concentrated the activator was the finer pores the specimen contained. It is also visible that S-4 and S-5 results were very similar and they seem to delimit maximum of the dependence from both sides. Samples S-6 and S-12 are not present in the following CFP results because they did not show any open-through porosity at all during

repeated measurements. Figure 12 illustrate a trend that clarifies that it is possible – samples S-4 and S-5 show a steep decrease in through-porosity at approximately 0.35 µm. The decrease is predictable because more dissolved matter between the particles, thus smaller pores, means of course a greater chance of clogging the channels through the porous body.

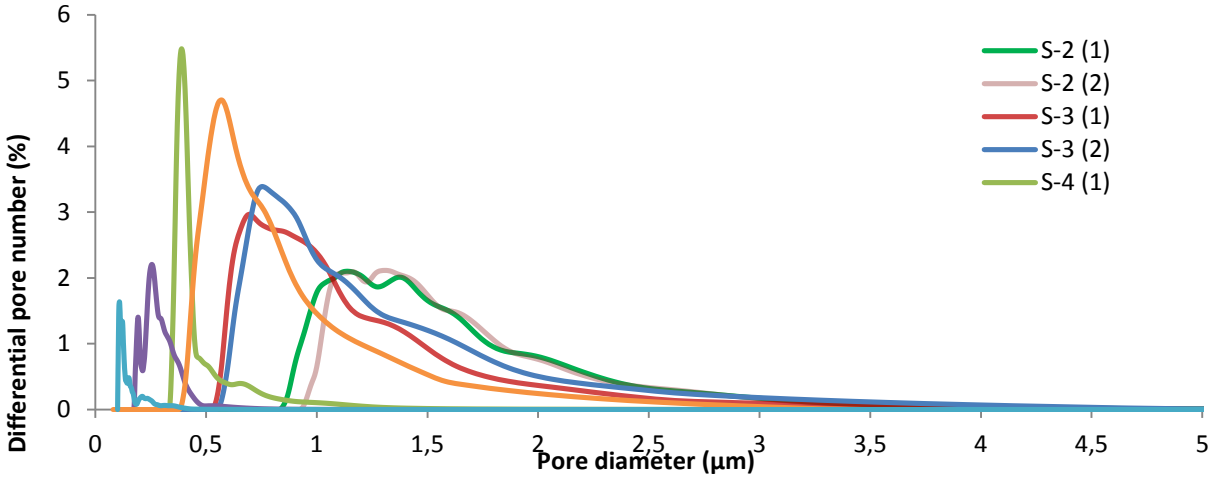

Figure 12: *CFP-based differential porosity curves of GGBFS samples*

The MIP results of the S series in the diagrams below confirm that both pore diameter and overall porosity decrease with the increasing activator concentration. The original $-dV/d(\log d)$ results from MIP, more precisely their maxima, show the trend more visibly then the differential pore number form in this case. Because this MIP-based porosity data seemed very promising but the differential form (which as all of these results is an average of 4 measurements) did not showed the curves in the expected order even after new series of samples was measured, it was decided to prepare new experimental series under greater pressure that could better regularize the particles. The pressure was set to twice the original one which was 1 ton for the barrier 25mm in diameter (that equals 19.5MPa) so this series was made under 2 tons (~ 39MPa). The results of MIP measurement of these samples can be seen in figures 64 and 65. The S-2 mixture proved to protrude from the row even more clearly than in the 1 ton series (Figures 62 and 63) and again it is more obvious from the $-dV/d(\log d)$ form of results. The total porosity decrease with increasing pressure can be seen on all samples (except the S-2 maxima). The standard deviation does not indicate that the S-2 results to be anyhow inconsistent or irrelevant within the series (Table 10).

Table 10: The average total porosity of the GGBFS samples with their standard deviations.

	S-1		S-2		S-3		S-4		S-5		S-6	
Pressure (Tons)	TP(%)	s.d.	TP(%)	s.d.	TP(%)	s.d.	TP(%)	s.d.	TP(%)	s.d.	TP(%)	s.d.
1	33.65	2.54	31.71	1.14	29.93	1.56	21.81	0.40	23.60	2.12	20.20	2.33
2	32.45	3.16	37.78	1.96	27.98	1.50	18.88	0.05	21.91	0.44	16.24	1.87

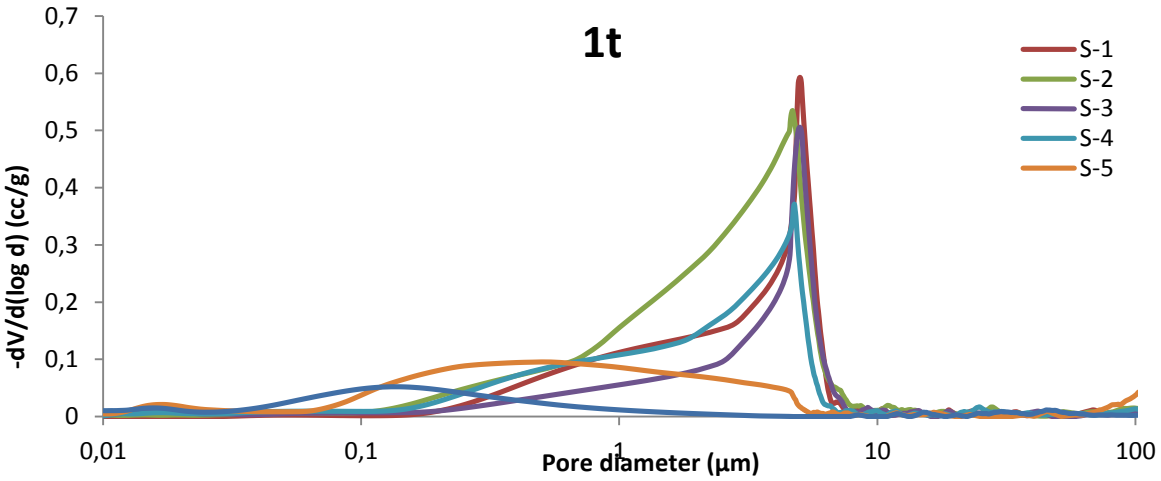

Figure 13: *MIP-based porosity measurements of GGBFS samples expressed in volume change of intruded mercury into certain pore diameter normalized to the sample weight*

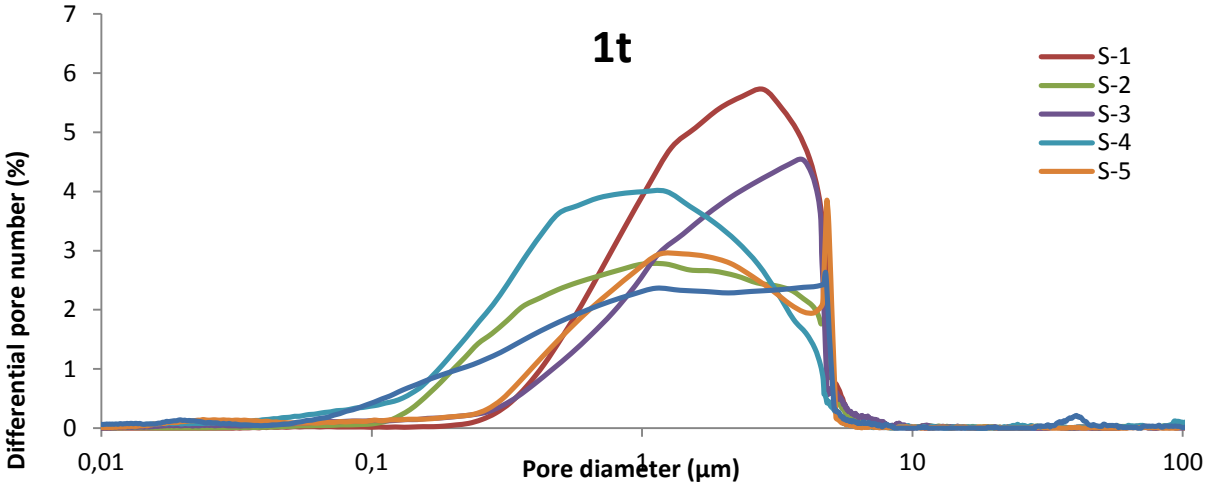

Figure 14: *MIP-based differential porosity measurements of GGBFS samples*

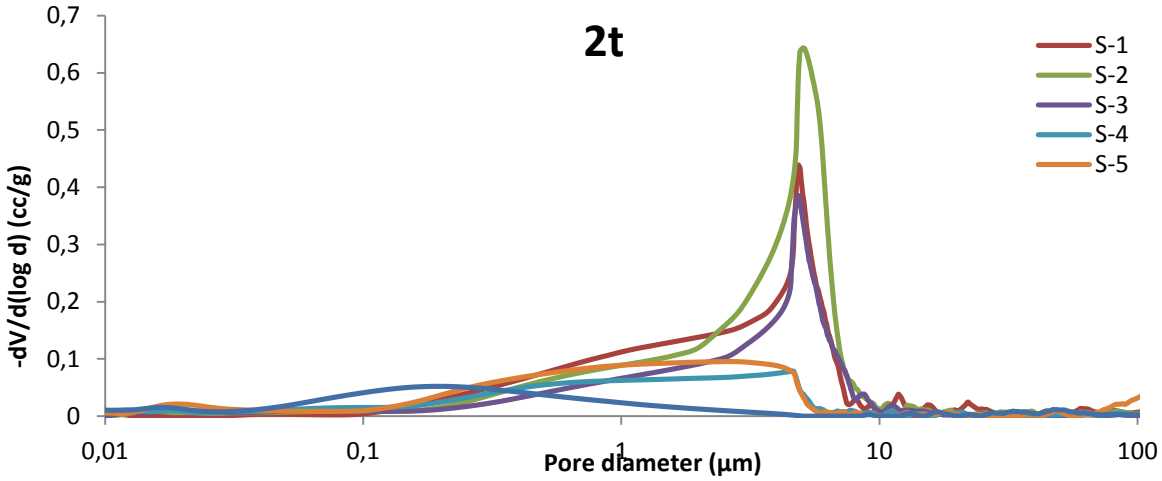

Figure 15: *MIP-based porosity measurements of GGBFS samples expressed in volume change of intruded mercury into certain pore diameter normalized to the sample weight*

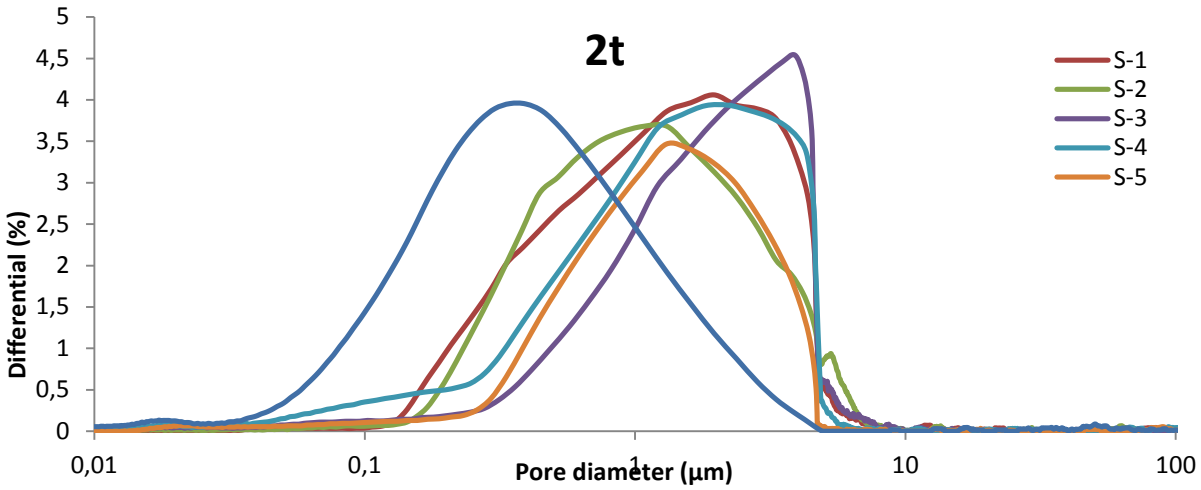

Figure 16: *MIP-based differential porosity measurements of GGBFS samples*

2.8 MICROSTRUCTURE

For SEM observations a small part of the specimens was taken and its cross-section smoothed with a sand paper and then polished using JEOL IB09010CP ionic polisher. Finally, samples were sputter-coated with gold and investigated by ZEISS EVO LS 10 scanning electron microscope in the mode of secondary electrons (SE) and back scattered electrons (BSE) detection. Accelerating voltage of the microscope was set to 10 kV.

Contacts between fly ash particles are evident from figures obtained by SEM, either in SE mode (Figure 17) or in BSE mode. At lower magnitude, differences in the FA-6 and FA-12 samples are not very clear at the first sight, but with a distance higher binding phase content is definite for higher dose of activator (observable at closer look in the form of rims around the fly ash grains). This fact is even for iron-rich particle, which is probably hematite or magnetite which is the brightest one in Figure 18, identified better below by EDS analysis in Figure 18. It can be expected that due to its composition such particle can hardly be alkali activated and it is thus likely that formation of binding phase around this particle was a consequence of dissolution of other particles.

It is generally accepted (Marjanović et al. 2015) that hydration product of alkaline activation of fly ash is sodium-aluminium-silicon-hydrate (N-A-S-H). Yet besides the original undisolved material inside the particles and N-A-S-H phase around and between them some crystals can be observed mainly near the borders of fly ash particles which meas some kinf of crystalic phase present in the samples.

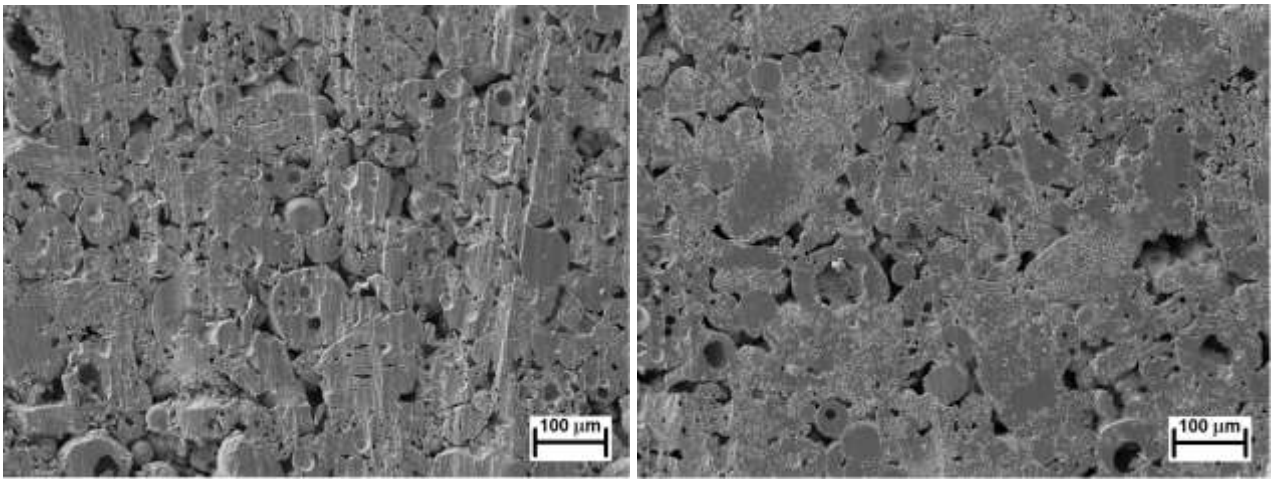

Figure 17: *Microstructure of the prepared specimens (FA 6 on the left and FA-12 on the right) observed by SEM in SE mode, magnitude 200×*

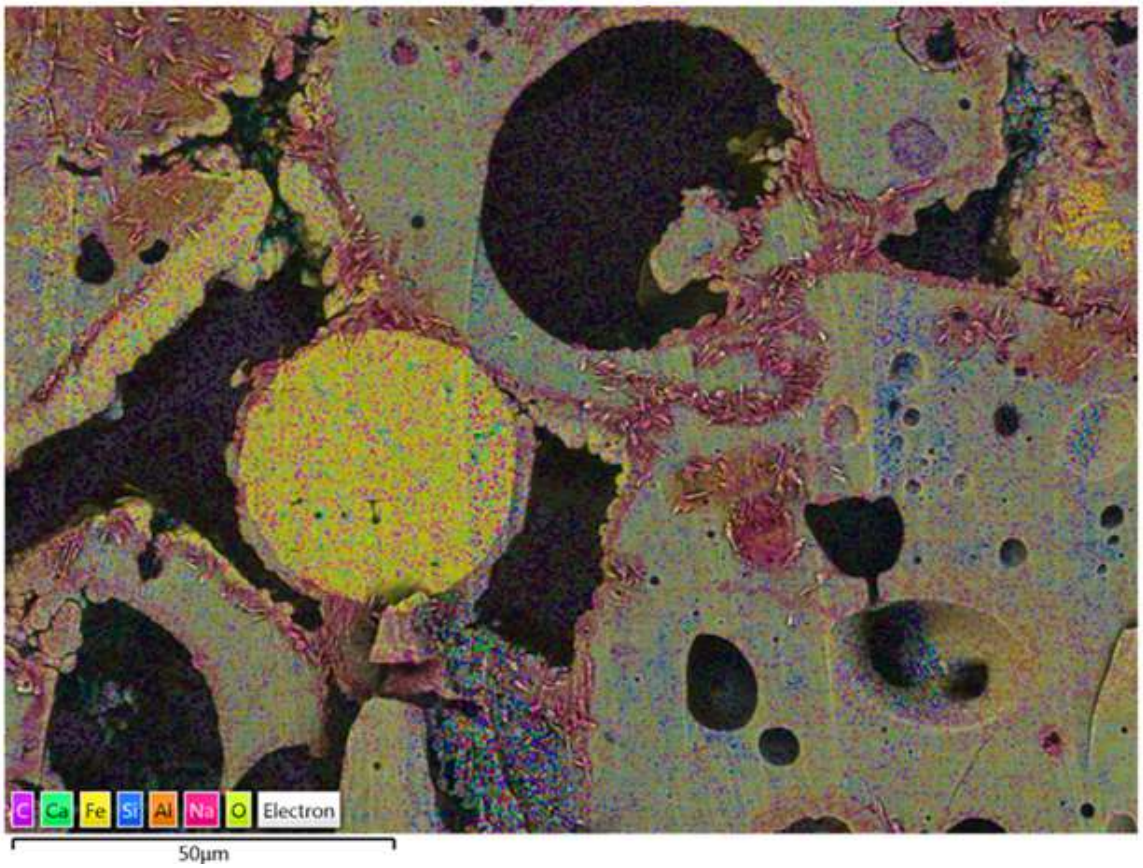

Figure 18: *Layered image made from the individual EDS analysis of FA-based specimen magnitude 2000×.*

The EDS revealed that the regions affected by crystal growth are rich in sodium and oxygen which was not a surprise and it can be therefore concluded that the crystals are pure sodium hydroxide. The only confusing fact for attentive person at this point is that the macroscopic crystals on the samples were of two different forms – round and opaque (what is typical for NaOH), and oblong and transparent. It was assumed that the second type has undergone the

carbonation process by picking up the atmospheric CO_2 while consuming the inner moisture during its growth to form sodium carbonate crystals.

To be sure, the crystals were scrubbed of the body to carry out the X-Ray powder Diffraction analysis (XRD) which confirmed that the crystals are sodium carbonate hydrate.

The BFS specimens were also investigated using SEM and the microstructure overview of the prepared membranes is given in Figure 19. There is also a comparison of barriers of the same composition prepared from unclassified slag to prove that the classification of the powders is necessary to obtain better porosity results. It can be seen that both types of membranes preserve porosity although it clearly illustrates that membranes based on unclassified GGBFS contain a lot of places where potentially larger pores are stuck by finer particles and thus number of desired pores decrease considerably. Moreover, microstructure of the membrane prepared from unclassified GGBFS is less homogenous compared to classified ones.

n the other hand increase in porosity is connected with decrease in strength and despite the fact that strength of unclassified-slag-based membranes was not investigated those prepared from classified GGBFS were more prone to cracking during the sample preparation and easier to abrade.

The main binding phase forming during alkaline activation of GGBFS is calcium-aluminium-silicate-hydrate (C-A-S-H) (Myers et al.,2013; Puertas et al. 2011). Thank to this phase, GGBFS grains are connected together and form filtration membrane (Figure 19). Its amount is sufficiently high to facilitate compactness of the body but it was low to satisfactorily determine its composition by EDS (see Figure 20). The micrographs however confirm that the GGBFS-based materials do not tend to effloresce because the crystals do not occur in them.

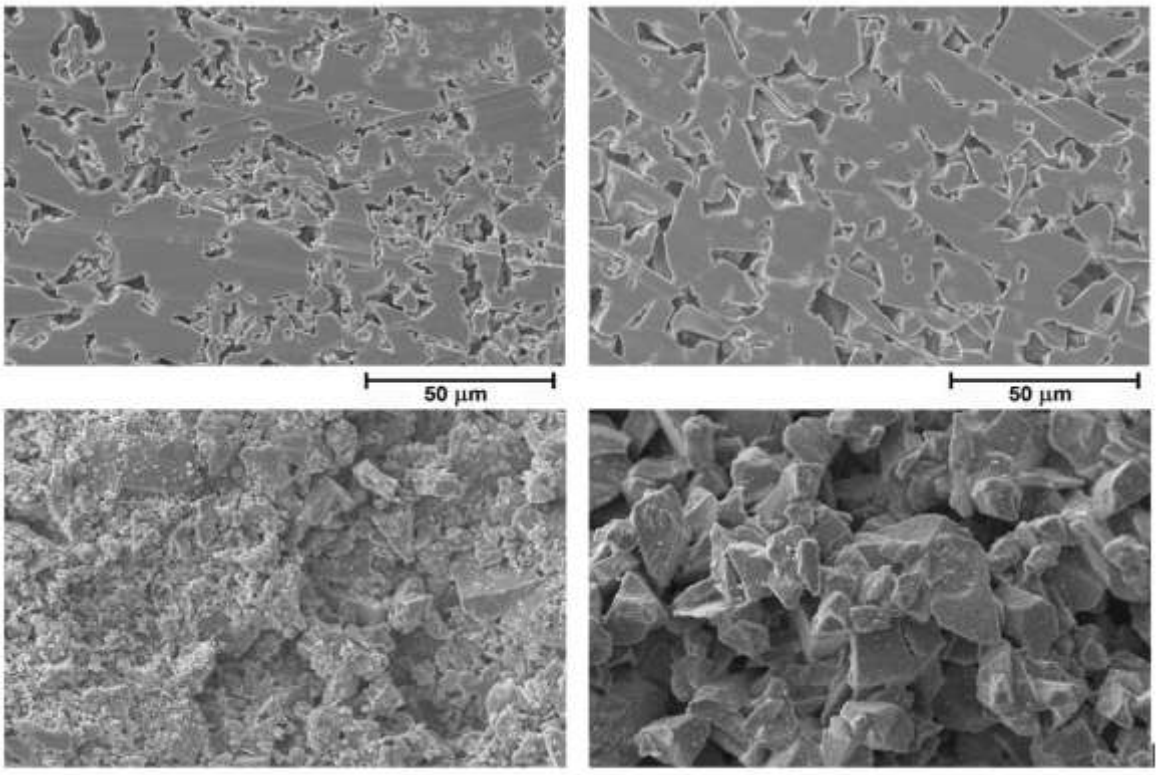

Figure 19: *Microstructure of polished (up) and unpolished (down) parts of the membrane from unclassified (left) and classified (right) GGBFS; magnitude 2 000×.*

Figure 20: *Layered image from the individual EDS analysis of GGBFS-based specimen.*

2.9 FINAL POROUS MATERIAL COMPOSITION

On the basis of the previous results and subsequent findings it was clear that the ideal mixture should have the SiO_2/Al_2O_3 ratio around 3, it should be based on GGBFS for the most part to be as strong as possible but contain minor part of FA and bauxite to reduce the GGBFS shrinkage and preserve the oxides ratio and it also has to be as dry as possible to maintain good porosity. After these conclusions the dataset of possible mixture compositions was searched through and one particular composition was chosen for the findings verification (the composition is listed in Table 11). The bodies from this material were prepared and the results of the mechanical and porosity tests as well as micrographs from SEM are listed below.

It is important to note at this point that with this level of dryness it is very difficult to mix the components well and obtain a homogenous structure. For good results the combination of manual mixing with planetary mixing machine treatment had to be applied and the machine mixing routine was amended to 5 times 15 seconds alternating with manual disruption of the material which tended to lodge to a firm aggregate in the mixing container under the planetary centrifugal motion.

Table 11: Composition and parameters of the final porous material X.

#	P1 (SiO_2/Al_2O_3)	P2 (Na_2O/Al_2O_3)	P3 (H_2O/Na_2O)	Glass	NaOH	Ash	Baux.	Slag	w/s
X	2.98	0.92	5.02	1.06	19.76	10.78	8.26	60.14	0.159

The material of this composition achieved in uniaxial tensile strength tests the results of 6.31 ± 0.20 MPa for the testing columns and 6.65 ± 0.49 MPa for the bodies grinded from the pressed barriers while maintaining very good level of fine porosity – see Figure 21 and for realistic idea of the material structure see Figure 22 showing ion beam polished sample.

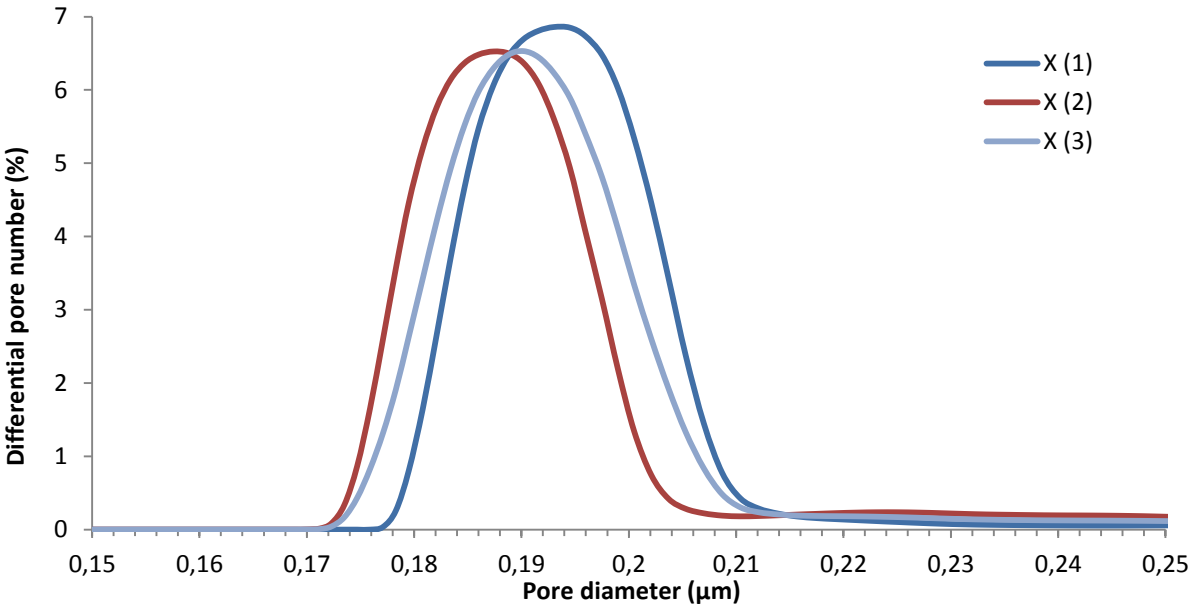

Figure 21: *CFP-based differential porosity curves of the X composition samples.*

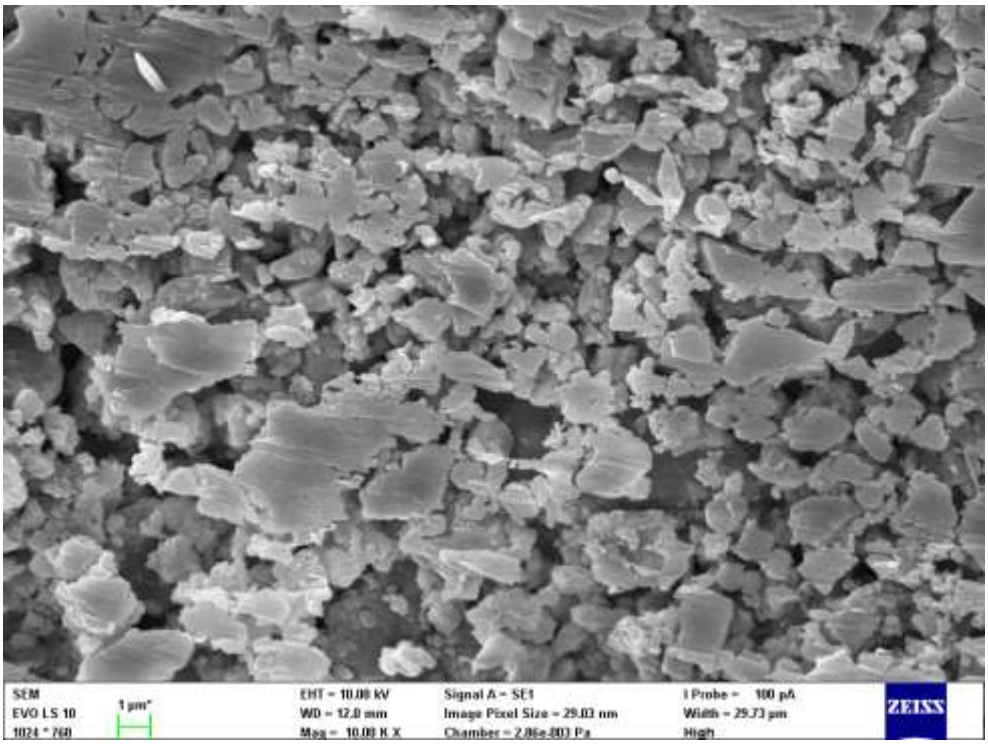

Figure 22: *SEM image of the X composition structure; magnitude 10000x.*

2.10 PERMEABILITY TESTING

After the strength and porosity of the final composition bodies were tested and the potential of the composition verified the permeability had to be proved using the filtration post. The first results had shown that the filtration barrier withstands even the maximal pressure of the filtration post (nearly 6 bar) but the uniform barrier of such pore-fineness to thickness ratio puts too much resistance to the flow and the permeability was only about 15 L/m^2.h.bar which correlate with the results in literature (Qin et al. 2015) but a lot less than the results of Fang et al. (2013) which was using asymmetrical filtration barriers so it was decided to prepare the barriers asymmetrically – coarser support with thin layer of the fine filtering material.

For the preparation of the coarser supporting layer an S-5 mixture analogue was chosen due to its best strength characteristics within the whole mixtures spectrum. The unground blast furnace slag had to be used and thus it had to be also classified. To cut the sharper fraction by classification of the powder ALPINE E200 LS air jet sieve with 125μm and 250μm sieves were used.

At first two different approaches were tested for the preparation – 'wet on wet' (pressing and curing two layers together while both freshly mixed) and 'wet on dry' (pressing the finer layer on fully hardened support). The issue with the readily hardened supports is that they tend to collapse under the pressing the finer mixture on top of them. The 'wet on wet' method had also a disadvantage which hides in an uneven thickness of the layers after pressing them, both soft, together. The results of these two approaches turned out not suitable and therefore the simple third technique was used in form of depositing the upper finer layer by laboratory spatula on the surface of the fully cured support, then cure it and sand off the surface to reduce its thickness and level the surface. The only issue of this method is that it is time consuming while measuring of the layer has to be done during the sanding to obtain comparable thicknesses on multiple pieces.

Regardless of the way of preparation the results of the asymmetrical barriers were different from each other because predictably the repeatability of the asymmetrical barriers made by hand is not perfect. The cured membranes made by the third above mentioned technique were then tested on the filtration post for permeability with water and the average results were 138 L/h.m^2.bar. Air permeability measured using Quantachrome 3Gzh porometer showed the permeability results of 1320 L/h.m^2.bar.

The results showed that the material is suitable for use in filtration media production. The only thing that remains to be resolved in the future is the optimization of the production procedures to improve the uniformity of the produced filtration barriers. Mainly the mechanism of application of the fine layer on top of the coarse layer is an issue. In ceramics this type of membrane could be manufactured via dipping the surface of the coarser support into the sludge or slurry of the fine material dispersed in water one or multiple times to build up an even and very thin layer. In this case though the mixture is necessarily in form of loose and lightly moist bulk material and further dilution would directly affect the mechanism of reaction and resulting mechanical properties. Therefore the deposition has to be done only mechanical way.

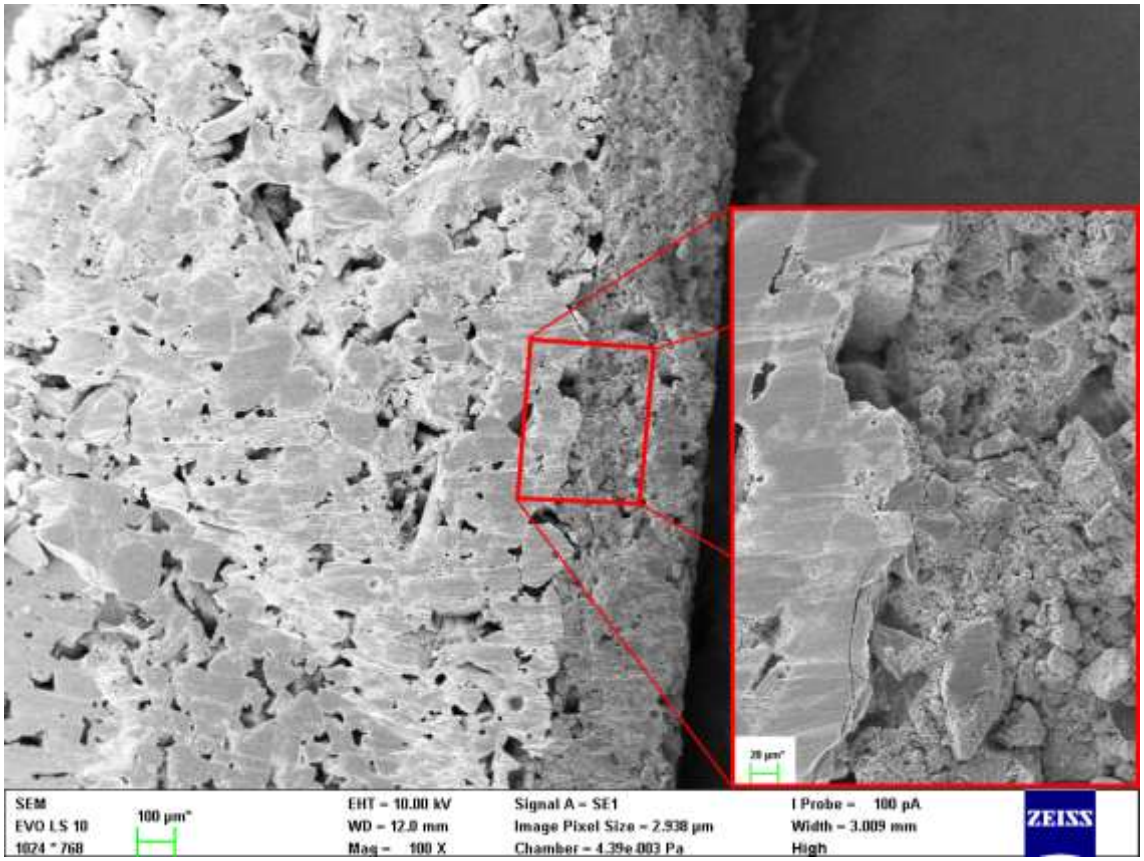

Figure 23: *Asymmetrical porous body SEM image; magnitude 100x + 500x cutout.*

By other means the overall practicability of the material seems very promising and with other sharp fractions segregated it can be applied similar to other inorganic filters, to tailor the filtration media of different pore diameters and overall geometries with emphasis on the particular application.

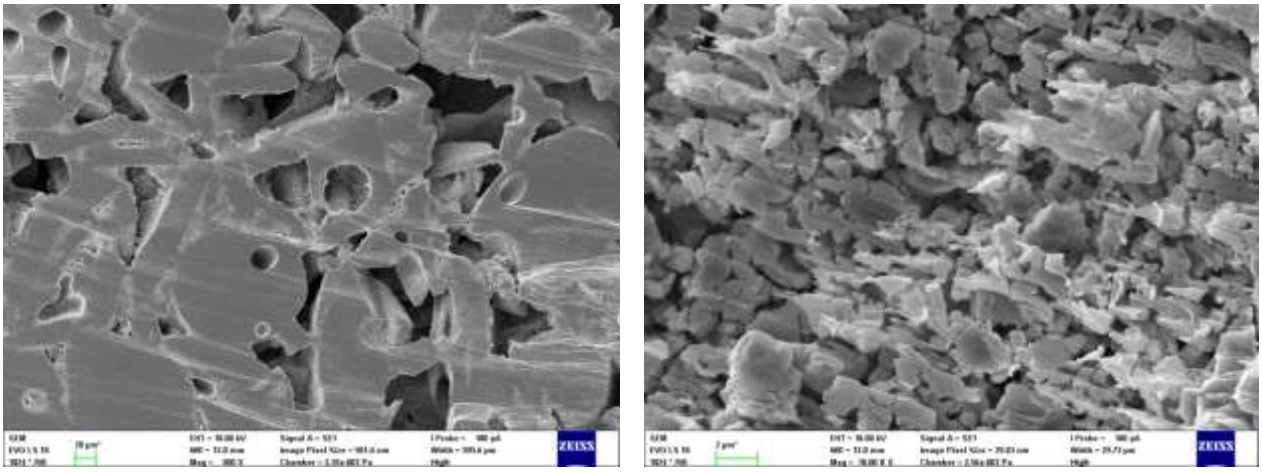

Figure 24: *Ion beam polished coarse supporting body structure(magnitude 500x) on the left and fine filtering layer(magnitude 10000x) on the right.*

3 DISCUSSION

The results of the study confirm that alkali activated secondary raw materials emphasizing blast furnace slag can be utilized to produce porous media with good strength parameters. The strength of the best porous materials prepared in the experimental part of the work are comparable to those of fly-ash based filtration membranes sintered at 800 °C du to literature (Singh et Bularasa, 2013).

Based on the strength results listed in this work, GGBFS seems to be more suitable for membrane material preparation than FA. However BFS issue when compared to FA is that its particles are angular, and when they are in contact with each other along their edges or walls, continuous porosity is reduced compared to round FA particles. On the other hand, through this principle GGBFS has a greater potential to build firmer links between the particles.

Understanding the main processes and patterns in the given alkali-activated materials' behavior led to the choice of one composition which could optimally combine strength and porosity. The composition chosen in this step was the driest possible one from the MATLAB-based dataset which combined the majority of the GGBFS to maintain the best strength, yet still maintained some of the fly ash and bauxite to preserve the best oxide ratios, better porosity and to reduce the inconsiderable shrinkage and tendency to crack while drying which the purely slag-based materials suffered from (Bílek et al., 2016). Addressing the shrinkage, the measurements showed that while purely FA-based bodies had, on average, a diameter of 25.55 mm after curing, purely slag-based samples' diameter was 25.36 mm, and the bodies made from the final mixture were 25.46 mm, which indicates a reduction in filter shrinkage by approximately half.

The data from the four-point uniaxial tensile tests of the columns made of various composition mixtures follow the regularities known for geopolymers. For the purpose of the work parameters P1 (SiO_2/Al_2O_3 ratio), P2 (Na_2O/Al_2O_3 ratio), P3 (H_2O/Na_2O ratio) and w/s (water to solids ratio) were established and the properties were observed from these parameters point of view.

The strength dependence on the SiO_2/Al_2O_3 ratio was proved to follow the precedent that, in the given range of approx. 2.7–3.2, the homogeneity of the material structure and thus its overall strength increases (and porosity decreases) with an increase in the ratio value corresponding to the results published by Duxson et al (2005).

The strong influence of the Na_2O/Al_2O_3 ratio on strength was verified in the strength results of the FA and S series of mixtures, which all have the same SiO_2/Al_2O_3 ratio within their groups. The Na_2O/Al_2O_3 ratio was very convincingly proved to show the best strength results when around unity as assumed based on the literature (Rowles et O'Connor, 2003; Duxson et al, 2005). In this case, the strength results do not match the conclusion that the concentration of the alkali activator for optimum strength of alkali activated BFS is 14 M (Singh et al, 2016). The literature-presented concentration is closest to composition S-4 (approx. 13.4M) but S-5 (approx. 16.2 M) had an 18% higher flexural strength than S-4.

The H_2O/M_2O ratio, that Kriven, Barbosa, Hos etc. had used for geopolymer characterization was found to be insufficient to characterize the material consistency and workability which was intended to be the main role of the parameter. Additionally, no visible dependence on the strength of the materials was observed due to the results, but it was not the main aim of this work so the compositions were not well-suited for the task. For ongoing work, the simple water to solids ratio (w/s) was adopted instead. This parameter was found to be the most appropriate for the workability characterization and in terms of final material strength influence was shown to be

important. The data show that within the examined w/s range, the strength of the final material decreases with an increase in the w/s ratio of the mixture.

The porosimetry measurements were performed via the MIP and CFP methods. The MIP method measures all opened pores, including dead-ends in the pore network, thus it better describes the overall nature of the material's porous structure. The CFP method is sensitive only to through-pores and better describes the permeability and potential filtering ability of the media. The results of the two methods therefore not only differ but show the porosity from two different perspectives. Both, however, mostly share the same final conclusions in terms of mixture-composition parameters to final material porosity dependencies for the FA and S series. Only in most cases one method shows it more visibly then the other. Both the FA and S series matched the assumption that by increasing the alkali activator concentration the strength increases significantly – in terms of porosity this means that pores are getting smaller, apparently due to the increasing ability of the activator to dissolve the surface layers of the particles and create thicker and thus stronger necks between them in the condensation stage. A downside of this process is that the material becomes more homogenous (with a greater amount of gepolymer gel, which binds the mass together) and the overall porosity thus decreases with the decrease in average pore diameter and also closure of many pores. The process of concentrating the alkali activator can be perceived as an increase in the sintering temperature of ceramics, which, also due to more material melting, creates wider and stronger necks between the particles but also decreases the porosity of the final product.

All of these facts make perfect sense when imagining the process on the scale of individual particles and wetting of their surface by the activator, which in a specific range of amounts only fills the spaces around the contact sites of the particles due to capillary drag and until a certain w/s limit the necks are only getting wider. It is, however, important to note that the range where this phenomenon occurs is specific to certain particles' granulometry, and even their morphology and the fluid ingredient resulting gel thickness. The overall importance of the finding is that this range should be always found in cases where the porosity of the final material is of interest and the amount of alkali activator should be optimized for the given case to create strong bonds but subvert the porosity as little as possible.

The SEM microphotographs show the necking phenomenon very clearly when comparing the pictures of classified raw material and the final AAM structure. The main factor which changes between them is the occurrence of necks bonding them together. Of course, with GGBFS the effect of smoothing the edges of the particles by etching caused by the alkali activator can also be observed in the unpolished surface micrographs.

One of the limitations of this study's results clarity is in one of its main focuses, the MATLAB computational mixture compositions. Although these were chosen to cover the intended range of values of all the parameters, they were mostly divergent in other variables. Then in certain cases their results do not follow the dependencies in the diagrams as clearly as they would if there were more series of samples compiled with only one variable changing through each of them. Without extensive understanding of the effects influencing the material properties, the diagrams of the MATLAB-designed series may seem disordered in some cases. Therefore, the otherwise unclear patterns were covered by designing the pure FA and S series, which plainly change only

the variables P2 (Na_2O/Al_2O_3 ratio) and P3 (H_2O/Na_2O ratio) to show the regularities in the observed properties they affect.

A second limitation is that the materials used (GGBFS and FA) may vary widely in composition depending on the factory they came from and also the production conditions. Every batch of blast furnace slag can differ which applies even more to every batch of fly ash that largely depends on the quality and composition of the coal used and the conditions it was burned in. This is, however, one of the reasons why it is very useful to utilize such instruments as the MATLAB calculation scheme when designing the AAM mixtures that takes the composition of the specific material into account and adapts the dose of every component accordingly.

The last thing to note was the manual compaction of the tensile testing columns when compared to the filtering barriers made by press molding under defined pressure, which translates to slightly different uniformity (and thus porosity and strength parameters) of the resulting bodies. The only other way to achieve the desired specimen cross section would be to apply the same pressure molding method (as with barriers) in a vertical oriented mold. This process was, however, found to be inapplicable due to high energy dissipation to the walls of the mold, causing very uneven longwise compaction of the samples. It was almost impossible to demold the columns without damaging them even though different types of mold separators and techniques were applied to improve the demolding process. The tensile testing columns were therefore made in ordinary dismountable molds by manual compaction. With such dry mixtures, however, the utilization of a vibrational stool would not properly compact the material, therefore the manual compaction was applied. Although the ultimate strength of the manually compacted columns may not exactly meet the strenght of press-molded bodies, the tensile testing results are a good indicator of the materials' mutual mechanical properties because the manual compaction procedure was normalized to increase the uniformity of the products as much as possible.

Addressing the final composition X, it must be said that approximately 7% of pores in the narrow distribution of approx. 0.19 μm in diameter from the CFP analysis may not seem very convincing. However, it is important to note that those are only the pores which go all the way through 2 mm-thick bodies, which gives an aspect ratio of 1:5,000 width to length of the through-pores (furthermore neglecting the tortuosity). This is of great importance and should be taken into consideration. This also applies to pores of the ambient widths (see Figure 21).

A fact that also plays a role is that the mixtures were spread manually across the molds and some regions were, unfortunately, more compacted than others. To verify this idea, some bodies from the same material were pressed under twice the pressure and they clearly showed significantly lower porosity. As a part of the conclusion it should therefore be noted that the production process should be further optimized, or, in the best case, automated to exploit better spreading, lower pressure, better uniformity and lower thicknesses. This would lead to a significant increase in the number of through-pores. This, however, is one of the suggestions for further research.

4 CONCLUSION

The aim of this work was to prepare and optimize inorganic porous media based on alkali-activated secondary raw materials to find out whether such material could be suitable for filtration praxis. The main reason for this research was that conventional inorganic materials use primary resources, a lot of energy and are thus more expensive and harmful to the environment.

The obvious goal of every filtration technique is to separate maximal quantum of one phase with minimal resistance to the other phase flow, because apart from the collection effectivity, one of the most important properties for every porous material used for filtration applications is its permeability. In general, a higher permeability can be obtained by either increasing the pore volume fraction, the pore size (which reduces the capture performance), or in best case increasing the pore-connectivity. It has to be also taken into account that the overall higher porosity always tend to impair the mechanical properties of the product. The optimization between porosity and mechanical strength is therefore always a key feature of filtration media design because it is impossible to obtain maximum values in both these factors. In this case the obtained through-porosity of the final material was good considering the fact that the filtration bodies' thicknesses were 4 orders of magnitude higher than the width of individual pores. The strength of the material of over 6 MPa is also perfectly acceptable.

The combination of a majority of GGBFS due to its better strength while bonded via alkali activation and minor fraction of FA due to the round shape of its particles, which properly complement the microstructure, seem very promising. Furthermore, it was observed that the FA admixture has the ability to reduce the unfavorable GGBFS shrinkage which was further proved by literature found later (Ye et Radlińska, 2016) and it possibly even improves the chemical resistance of the final material (Pařízek et al, 2016).

The idea for the topic of this work and its main aim came from the fact that contemporary inorganic porous materials share the same principle – connecting particles of inorganic material together to form a porous structure of certain properties, only each of them different way. But why to use primary resources which are more and more precious, expensive and need an extra step which consumes a lot of energy (e.g. sintering ceramics or clinker production)? Fly ash and blast furnace slag, even already used in a few applications, are still high-volume industrial wastes but because they possess favorable properties in the form of their pozzolanic activity, should be utilized much more to avoid the practice of landfilling them without further attention and consuming more primary resources instead.

Partial objectives of the work were sufficiently met with available resources. The first – to demonstrate a low-cost method for making porous filter media accompanied the whole work and the only issue is that for future utilization, some level of automation of spreading out and pressing the material is needed to obtain even better values and repeatability of the results.

Second partial aim was to tailor the pore microstructure by varying the content and size of ingredients. This objective was met by fractionation of the ingredients and varying their content into various mixtures due to very robust experimental design based on calculation rather than tentative determination of the compositions.

The third and fourth partial aims were to affect the pore microstructure with attention to permeability and with attention to mechanical strength. These two objectives have clearly contradictory goals but share the main idea of porous structure research – to find an optimum in

which the porosity and strength of the final material meet in the best ratio within the preset conditions. The optimal zone of the investigated AAM strength and porosity was found to be shifted towards the BFS, although the FA admixture (along with bauxite) still plays an important role in the system.

The last partial aim was to illustrate a novel filtration material which is both fast and effective, which the final composition of the alkali-activated mixtures is perfectly capable of accomplishing with sufficiently developed technology for the barriers preparation. The microstructure of the material looks very promising and the level of strength the material exhibits with that level of porosity is very good. The issue and subject for further research is to prepare the membrane (from this kind of very dry mixture) sufficiently thin in order to verify the filtration properties of such barriers in practical applications.

5 REFERENCES

AZARSHAB, Mohammadreza, Farzaneh MOHAMMADI, Hojjatollah MAGHSOODLOORAD a Toraj MOHAMMADI. Ceramic membrane synthesis based on alkali activated blast furnace slag for separation of water from ethanol. Ceramics International [online]. 2016, 42(14), 15568-15574 [cit. 2018-06-06]. DOI: 10.1016/j.ceramint.2016.07.005. ISSN 02728842. Dostupné z: http://linkinghub.elsevier.com/retrieve/pii/S0272884216310598

BAKHAREV, T. Geopolymeric materials prepared using Class F fly ash and elevated temperature curing. Cement and Concrete Research [online]. 2005, 35(6), 1224-1232 [cit. 2018-04-30]. DOI: 10.1016/j.cemconres.2004.06.031. ISSN 00088846. Dostupné z: http://linkinghub.elsevier.com/retrieve/pii/S0008884604002844

BARBOSA, Valeria F.F, Kenneth J.D MACKENZIE a Clelio THAUMATURGO. Synthesis and characterisation of materials based on inorganic polymers of alumina and silica: sodium polysialate polymers. International Journal of Inorganic Materials [online]. 2000, 2(4), 309-317 [cit. 2018-05-29]. DOI: 10.1016/S1466-6049(00)00041-6. ISSN 14666049. Dostupné z: http://linkinghub.elsevier.com/retrieve/pii/S1466604900000416

BÍLEK, Vlastimil, Lukáš KALINA, Radoslav NOVOTNÝ, Jakub TKACZ a Ladislav PAŘÍZEK. Some Issues of Shrinkage-Reducing Admixtures Application in Alkali-Activated Slag Systems. Materials [online]. 2016, 9(6), 462- [cit. 2018-04-30]. DOI: 10.3390/ma9060462. ISSN 1996-1944. Dostupné z: http://www.mdpi.com/1996-1944/9/6/462

BILIM, Cahit, Okan KARAHAN, Cengiz Duran ATIŞ a Serhan İLKENTAPAR. Effects of chemical admixtures and curing conditions on some properties of alkali-activated cementless slag mixtures. KSCE Journal of Civil Engineering [online]. 2015, 19(3), 733-741 [cit. 2018-04-30]. DOI: 10.1007/s12205-015-0629-0. ISSN 1226-7988. Dostupné z: http://link.springer.com/10.1007/s12205-015-0629-0

BILIM, Cahit, Okan KARAHAN, Cengiz Duran ATIŞ a Serhan İLKENTAPAR. Influence of admixtures on the properties of alkali-activated slag mortars subjected to different curing conditions. Materials & Design [online]. 2013, 44, 540-547 [cit. 2018-04-30]. DOI: 10.1016/j.matdes.2012.08.049. ISSN 02613069. Dostupné z: http://linkinghub.elsevier.com/retrieve/pii/S0261306912005882

CAO, Jingjie, Xinfa DONG, Lingling LI, Yingchao DONG a Stuart HAMPSHIRE. Recycling of waste fly ash for production of porous mullite ceramic membrane supports with increased porosity. Journal of the European Ceramic Society [online]. 2014, 34(13), 3181-3194 [cit. 2018-06-02]. DOI: 10.1016/j.jeurceramsoc.2014.04.011. ISSN 09552219. Dostupné z: http://linkinghub.elsevier.com/retrieve/pii/S095522191400199X

DAVIDOVITS, Joseph. 2008. *Geopolymer: chemistry*. 2nd ed. Saint-Quentin: Institute Géopolymère, 587 s. ISBN 29-514-8201-9.

DUAN, Ping, Chunjie YAN, Wei ZHOU a Daming REN. Development of fly ash and iron ore tailing based porous geopolymer for removal of Cu(II) from wastewater. Ceramics International [online]. 2016, 42(12), 13507-13518 [cit. 2018-06-06]. DOI: 10.1016/j.ceramint.2016.05.143. ISSN 02728842. Dostupné z: http://linkinghub.elsevier.com/retrieve/pii/S0272884216307490

DUXSON, Peter, John L. PROVIS, Grant C. LUKEY, Seth W. MALLICOAT, Waltraud M. KRIVEN a Jannie S.J. VAN DEVENTER. Understanding the relationship between geopolymer composition, microstructure and mechanical properties. Colloids and Surfaces A: Physicochemical and Engineering Aspects [online]. 2005, 269(1-3), 47-58 [cit. 2018-05-28]. DOI: 10.1016/j.colsurfa.2005.06.060. ISSN 09277757. Dostupné z: http://linkinghub.elsevier.com/retrieve/pii/S0927775705004966

FANG, Jing, Guotong QIN, Wei WEI, Xinqing ZHAO a Lei JIANG. Elaboration of new ceramic membrane from spherical fly ash for microfiltration of rigid particle suspension and oil-in-water emulsion. Desalination [online]. 2013, 311, 113-126 [cit. 2018-04-30]. DOI: 10.1016/j.desal.2012.11.008. ISSN 00119164. Dostupné z: http://linkinghub.elsevier.com/retrieve/pii/S0011916412006030

HENON, Joseph, Arnaud ALZINA, Joseph ABSI, David Stanley SMITH, Sylvie ROSSIGNOL a S. ROSSIGNOL. 2012. Porosity control of cold consolidated geomaterial foam: Temperature effect. *Ceramics International*. 38(1): 77-84. DOI: 10.1016/j.ceramint.2011.06.040. ISSN 02728842. Dostupné z: http://linkinghub.elsevier.com/retrieve/pii/S0272884211005827

HARDJITO, Djwantoro, Steenie E. WALLAH, Dody M. J. SUMAJOUW a Rangan B. V. Factors Influencing the Compressive Strength of Fly ash-Based Geopolymer Concrete. In: Civil Engineering Dimension. Vol. 6, No. 2. 2004, s. 88-93. DOI: 10.9744/ced.6.2.pp.%2088-93. ISSN 1410-9530.

HARDJITO, Djwantoro, Chua Chung CHEAK a Carrie Ho LEE ING. Strength and Setting Times of Low Calcium Fly Ash-based Geopolymer Mortar. Modern Applied Science [online]. 2009, 2(4), - [cit. 2018-04-30]. DOI: 10.5539/mas.v2n4p3. ISSN 1913-1852. Dostupné z: http://www.ccsenet.org/journal/index.php/mas/article/view/2403

JEDIDI, Ilyes, Sabeur KHEMAKHEM, Sami SAÏDI, et al. Preparation of a new ceramic microfiltration membrane from mineral coal fly ash: Application to the treatment of the textile dying effluents. Powder Technology [online]. 2011, 208(2), 427-432 [cit. 2018-03-14]. DOI: 10.1016/j.powtec.2010.08.039. ISSN 00325910. Dostupné z: http://linkinghub.elsevier.com/retrieve/pii/S0032591010004316

JO, Y.M., R. HUCHISON a J.A. RAPER. Preparation of Ceramic Membrane Filters, From Waste Fly Ash, Suitable for Hot Gas Cleaning. Waste Management & Research [online]. 1996, 14(3), 281-295 [cit. 2018-04-30]. DOI: 10.1177/0734242X9601400304. ISSN 0734-242X. Dostupné z: http://journals.sagepub.com/doi/10.1177/0734242X9601400304

KAUR, Mandeep, Jaspal SINGH a Manpreet KAUR. Synthesis of fly ash based geopolymer mortar considering different concentrations and combinations of alkaline activator solution. Ceramics International[online]. 2018, 44(2), 1534-1537 [cit. 2018-03-14]. DOI: 10.1016/j.ceramint.2017.10.071. ISSN 02728842. Dostupné z: http://linkinghub.elsevier.com/retrieve/pii/S0272884217322630

KIM, Min Sik, Yubin JUN, Changha LEE a Jae Eun OH. Use of CaO as an activator for producing a price-competitive non-cement structural binder using ground granulated blast furnace slag. Cement and Concrete Research [online]. 2013, 54, 208-214 [cit. 2018-03-14]. DOI: 10.1016/j.cemconres.2013.09.011. ISSN 00088846. Dostupné z: http://linkinghub.elsevier.com/retrieve/pii/S000888461300197X

KONG, Daniel L.Y. a Jay G. SANJAYAN. Damage behavior of geopolymer composites exposed to elevated temperatures. Cement and Concrete Composites [online]. 2008, 30(10), 986-991 [cit. 2018-05-21]. DOI: 10.1016/j.cemconcomp.2008.08.001. ISSN 09589465. Dostupné z: http://linkinghub.elsevier.com/retrieve/pii/S0958946508001005

LANDI, Elena, Valentina MEDRI, Elettra PAPA, Jiri DEDECEK, Petr KLEIN, Patricia BENITO a Angelo VACCARI. 2013. Alkali-bonded ceramics with hierarchical tailored porosity. *Applied Clay Science*. Hoboken, NJ, USA: John Wiley, 73(6): 56-64. DOI: 10.1016/j.clay.2012.09.027. ISBN 0471266965. ISSN 01691317. Dostupné z: http://linkinghub.elsevier.com/retrieve/pii/S0169131712002578

LEE, N.K., Hammad R. KHALID a H.K. LEE. Adsorption characteristics of cesium onto mesoporous geopolymers containing nano-crystalline zeolites. Microporous and Mesoporous Materials [online]. 2017, 242, 238-244 [cit. 2018-04-30]. DOI: 10.1016/j.micromeso.2017.01.030. ISSN 13871811. Dostupné z: http://linkinghub.elsevier.com/retrieve/pii/S1387181117300306

LEE, Yu-Ri, June Thet SOE, Siqian ZHANG, Ji-Whan AHN, Min Bum PARK a Wha-Seung AHN. Synthesis of nanoporous materials via recycling coal fly ash and other solid wastes: A mini review. Chemical Engineering Journal [online]. 2017B, 317, 821-843 [cit. 2018-05-21]. DOI: 10.1016/j.cej.2017.02.124. ISSN 13858947. Dostupné z: http://linkinghub.elsevier.com/retrieve/pii/S1385894717302899

MARJANOVIĆ, N., M. KOMLJENOVIĆ, Z. BAŠČAREVIĆ, V. NIKOLIĆ a R. PETROVIĆ. Physical–mechanical and microstructural properties of alkali-activated fly ash–blast furnace slag blends. Ceramics International [online]. 2015, 41(1), 1421-1435 [cit. 2018-04-30]. DOI:

10.1016/j.ceramint.2014.09.075. ISSN 02728842. Dostupné z: http://linkinghub.elsevier.com/retrieve/pii/S0272884214014606

MEDPELLI, Dinesh, Jung-Min SEO, Dong-Kyun SEO a F. GLASSER. Geopolymer with Hierarchically Meso-/Macroporous Structures from Reactive Emulsion Templating. Journal of the American Ceramic Society [online]. 2014, 97(1), 70-73 [cit. 2018-06-02]. DOI: 10.1111/jace.12724. ISSN 00027820. Dostupné z: http://doi.wiley.com/10.1111/jace.12724

MEMON, Fareed Ahmed, Muhd Fadhil NURUDDIN, Samuel DEMIE a Nasir SHAFIQ. Effect of Curing Conditions on Strength of Fly ash-based Self-Compacting Geopolymer Concrete. Construction and Architectural Engineering. 2011, 5(8), 1-4. DOI: doi.org/10.5281/zenodo.1070949.

MOHAMMADI, Farzaneh a Toraj MOHAMMADI. Optimal conditions of porous ceramic membrane synthesis based on alkali activated blast furnace slag using Taguchi method. Ceramics International [online]. 2017, 43(16), 14369-14379 [cit. 2018-06-06]. DOI: 10.1016/j.ceramint.2017.07.197. ISSN 02728842. Dostupné z: http://linkinghub.elsevier.com/retrieve/pii/S0272884217316450

MYERS, Rupert J., Susan A. BERNAL, Rackel SAN NICOLAS a John L. PROVIS. Generalized Structural Description of Calcium–Sodium Aluminosilicate Hydrate Gels: The Cross-Linked Substituted Tobermorite Model. Langmuir [online]. 2013, 29(17), 5294-5306 [cit. 2018-04-30]. DOI: 10.1021/la4000473. ISSN 0743-7463. Dostupné z: http://pubs.acs.org/doi/10.1021/la4000473

NASVI, M.C.M., P.G. RANJITH, J. SANJAYAN, J.-M. CLACENS, S. ARII-CLACENS, I. SOBRADOS, C. PEYRATOUT, A. SMITH, J. SANZ, et al. 2013. The permeability of geopolymer at down-hole stress conditions: Application for carbon dioxide sequestration wells. *Applied Energy*. 102(21): 1391-1398. DOI: 10.1016/j.apenergy.2012.09.004. ISSN 03062619. Dostupné z: http://linkinghub.elsevier.com/retrieve/pii/S0306261912006447

NASVI, M.C.M., P.G. RANJITH, J. SANJAYAN a H. BUI. 2014. Effect of temperature on permeability of geopolymer: A primary well sealant for carbon capture and storage wells. *Fuel*. 117: 354-363. DOI: 10.1016/j.fuel.2013.09.007. ISSN 00162361. Dostupné z: http://linkinghub.elsevier.com/retrieve/pii/S0016236113008363

NEDELJKOVIĆ, Marija, Branko ŠAVIJA, Yibing ZUO, Mladena LUKOVIĆ a Guang YE. Effect of natural carbonation on the pore structure and elastic modulus of the alkali-activated fly ash and slag pastes. Construction and Building Materials [online]. 2018, 161, 687-704 [cit. 2018-06-11]. DOI: 10.1016/j.conbuildmat.2017.12.005. ISSN 09500618. Dostupné z: http://linkinghub.elsevier.com/retrieve/pii/S0950061817324005

NEMATOLLAHI, Behzad a Jay SANJAYAN. Effect of different superplasticizers and activator combinations on workability and strength of fly ash based geopolymer. Materials & Design [online]. 2014, 57, 667-672 [cit. 2018-05-21]. DOI: 10.1016/j.matdes.2014.01.064. ISSN 02613069. Dostupné z: http://linkinghub.elsevier.com/retrieve/pii/S0261306914000934

NIKLIOĆ, I., S. MARKOVIĆ, I. JANKOVIĆ – ČASTVAN, V.V. RADMILOVIĆ, Lj. KARANOVIĆ, Biljana BABIĆ a V.R. RADMILOVIĆ. Modification of mechanical and thermal properties of fly ash-based geopolymer by the incorporation of steel slag. Materials Letters [online]. 2016, 176, 301-305 [cit. 2018-06-06]. DOI: 10.1016/j.matlet.2016.04.121. ISSN 0167577X. Dostupné z: http://linkinghub.elsevier.com/retrieve/pii/S0167577X16306267

PAŘÍZEK, Ladislav, Vlastimil BÍLEK a Matěj BŘEZINA. Chloride Resistance of Alkali Activated Slag Pastes with Fly Ash Replacement. Materials Science Forum [online]. 2016, 851, 98-103 [cit. 2018-03-13]. DOI: 10.4028/www.scientific.net/MSF.851.98. ISSN 1662-9752. Dostupné z: http://www.scientific.net/MSF.851.98

PHAIR, J.W., J.S.J. VAN DEVENTER a J.D. SMITH. Effect of Al source and alkali activation on Pb and Cu immobilisation in fly-ash based "geopolymers". Applied Geochemistry [online]. 2004, 19(3), 423-434 [cit. 2018-06-06]. DOI: 10.1016/S0883-2927(03)00151-3. ISSN 08832927. Dostupné z: http://linkinghub.elsevier.com/retrieve/pii/S0883292703001513

PRUD'HOMME, E., P. MICHAUD, E. JOUSSEIN, C. PEYRATOUT, A. SMITH, S. ARRII-CLACENS, J.M. CLACENS a S. ROSSIGNOL. 2010. Silica fume as porogent agent in geo-materials at low temperature: A review. *Journal of the European Ceramic Society*. 30(7): 307-315. DOI: 10.1016/j.jeurceramsoc.2010.01.014. ISSN 09552219. Dostupné z: http://linkinghub.elsevier.com/retrieve/pii/S0272884213006573

PRUD'HOMME, E., P. MICHAUD, E. JOUSSEIN, C. PEYRATOUT, A. SMITH a S. ROSSIGNOL. 2011A. In situ inorganic foams prepared from various clays at low temperature. *Applied Clay Science*. 51(1-2): 15-22. DOI: 10.1016/j.clay.2010.10.016. ISSN 01691317. Dostupné z: http://linkinghub.elsevier.com/retrieve/pii/S0169131710003443

PRUD'HOMME, E., P. MICHAUD, E. JOUSSEIN, J.-M. CLACENS, S. ARII-CLACENS, I. SOBRADOS, C. PEYRATOUT, A. SMITH, J. SANZ, et al. 2011B. Structural characterization of geomaterial foams — Thermal behavior: A review. *Journal of Non-Crystalline Solids*. 357(21): 3637-3647. DOI: 10.1016/j.jnoncrysol.2011.06.033. ISSN 00223093. Dostupné z: http://linkinghub.elsevier.com/retrieve/pii/S0022309311004418

PUERTAS, F., M. PALACIOS, H. MANZANO, J.S. DOLADO, A. RICO a J. RODRÍGUEZ. A model for the C-A-S-H gel formed in alkali-activated slag cements. Journal of the European Ceramic Society [online]. 2011, 31(12), 2043-2056 [cit. 2018-04-30]. DOI:

10.1016/j.jeurceramsoc.2011.04.036. ISSN 09552219. Dostupné z: http://linkinghub.elsevier.com/retrieve/pii/S0955221911002159

PUERTAS, F., C. VARGA a M.M. ALONSO. Rheology of alkali-activated slag pastes. Effect of the nature and concentration of the activating solution. Cement and Concrete Composites [online]. 2014, 53, 279-288 [cit. 2018-03-14]. DOI: 10.1016/j.cemconcomp.2014.07.012. ISSN 09589465. Dostupné z: http://linkinghub.elsevier.com/retrieve/pii/S0958946514001309

QIN, Guotong, Xueqian LÜ, Wei WEI, Jiajia LI, Ruyue CUI a Shixuan HU. Microfiltration of kiwifruit juice and fouling mechanism using fly-ash-based ceramic membranes. Food and Bioproducts Processing [online]. 2015, 96, 278-284 [cit. 2018-04-30]. DOI: 10.1016/j.fbp.2015.09.006. ISSN 09603085. Dostupné z: http://linkinghub.elsevier.com/retrieve/pii/S0960308515001157

ROVNANÍK, Pavel. Effect of curing temperature on the development of hard structure of metakaolin-based geopolymer. Construction and Building Materials [online]. 2010, 24(7), 1176-1183 [cit. 2018-04-30]. DOI: 10.1016/j.conbuildmat.2009.12.023. ISSN 09500618. Dostupné z: http://linkinghub.elsevier.com/retrieve/pii/S0950061809004346

ROWLES, Matthew R. a Brian H. O'CONNOR. Chemical and Structural Microanalysis of Aluminosilicate Geopolymers Synthesized by Sodium Silicate Activation of Metakaolinite. Journal of the American Ceramic Society [online]. 2009, 92(10), 2354-2361 [cit. 2018-05-28]. DOI: 10.1111/j.1551-2916.2009.03191.x. ISSN 00027820. Dostupné z: http://doi.wiley.com/10.1111/j.1551-2916.2009.03191.x

RUNTTI, Hanna, Tero LUUKKONEN, Mikko NISKANEN, et al. Sulphate removal over barium-modified blast-furnace-slag geopolymer. Journal of Hazardous Materials [online]. 2016, 317, 373-384 [cit. 2018-04-30]. DOI: 10.1016/j.jhazmat.2016.06.001. ISSN 03043894. Dostupné z: http://linkinghub.elsevier.com/retrieve/pii/S0304389416305568

SAKULICH, A. R. a D. P. BENTZ. Mitigation of autogenous shrinkage in alkali activated slag mortars by internal curing. Materials and Structures [online]. 2013, 46(8), 1355-1367 [cit. 2018-04-30]. DOI: 10.1617/s11527-012-9978-z. ISSN 1359-5997. Dostupné z: http://link.springer.com/10.1617/s11527-012-9978-z

SARKER, Prabir Kumar, Sean KELLY a Zhitong YAO. 2014. Effect of fire exposure on cracking, spalling and residual strength of fly ash geopolymer concrete. *Materials*. 63: 584-592. DOI: 10.1016/j.matdes.2014.06.059. ISSN 02613069. Dostupné z: http://linkinghub.elsevier.com/retrieve/pii/S0261306914005147

SCHNEIDER, M., M. ROMER, M. TSCHUDIN a H. BOLIO. Sustainable cement production—present and future. Cement and Concrete Research [online]. 2011, 41(7), 642-650

[cit. 2018-05-21]. DOI: 10.1016/j.cemconres.2011.03.019. ISSN 00088846. Dostupné z: http://linkinghub.elsevier.com/retrieve/pii/S0008884611000950

SINGH, Gurpreet a Vijaya Kumar BULASARA. Preparation of low-cost microfiltration membranes from fly ash. Desalination and Water Treatment [online]. 2013, , 1-9 [cit. 2018-04-30]. DOI: 10.1080/19443994.2013.855677. ISSN 1944-3994. Dostupné z: http://www.tandfonline.com/doi/abs/10.1080/19443994.2013.855677

SINGH, B., M.R. RAHMAN, R. PASWAN a S.K. BHATTACHARYYA. Effect of activator concentration on the strength, ITZ and drying shrinkage of fly ash/slag geopolymer concrete. Construction and Building Materials [online]. 2016, 118, 171-179 [cit. 2018-03-14]. DOI: 10.1016/j.conbuildmat.2016.05.008. ISSN 09500618. Dostupné z: http://linkinghub.elsevier.com/retrieve/pii/S0950061816307267

TEMUUJIN, J., R.P. WILLIAMS a A. VAN RIESSEN. Effect of mechanical activation of fly ash on the properties of geopolymer cured at ambient temperature. Journal of Materials Processing Technology [online]. 2009, 209(12-13), 5276-5280 [cit. 2018-05-21]. DOI: 10.1016/j.jmatprotec.2009.03.016. ISSN 09240136. Dostupné z: http://linkinghub.elsevier.com/retrieve/pii/S0924013609001058

TEWARI, P.K., R.K. SINGH, V.S. BATRA a M. BALAKRISHNAN. Membrane bioreactor (MBR) for wastewater treatment: Filtration performance evaluation of low cost polymeric and ceramic membranes. Separation and Purification Technology [online]. 2010, 71(2), 200-204 [cit. 2018-06-02]. DOI: 10.1016/j.seppur.2009.11.022. ISSN 13835866. Dostupné z: http://linkinghub.elsevier.com/retrieve/pii/S1383586609004791

THO-IN, Tawatchai, Vanchai SATA, Prinya CHINDAPRASIRT a Chai JATURAPITAKKUL. Pervious high-calcium fly ash geopolymer concrete. Construction and Building Materials [online]. 2012, 30, 366-371 [cit. 2018-05-21]. DOI: 10.1016/j.conbuildmat.2011.12.028. ISSN 09500618. Dostupné z: http://linkinghub.elsevier.com/retrieve/pii/S0950061811007057

VAN JAARSVELD, J.G.S., J.S.J. VAN DEVENTER a L. LORENZEN. The potential use of geopolymeric materials to immobilise toxic metals: Part I. Theory and applications. Minerals Engineering [online]. 1997, 10(7), 659-669 [cit. 2018-06-06]. DOI: 10.1016/S0892-6875(97)00046-0. ISSN 08926875. Dostupné z: http://linkinghub.elsevier.com/retrieve/pii/S0892687597000460

VAN JAARSVELD, J.G.S, J.S.J VAN DEVENTER a G.C LUKEY. The effect of composition and temperature on the properties of fly ash- and kaolinite-based geopolymers. Chemical Engineering Journal [online]. 2002, 89(1-3), 63-73 [cit. 2018-04-30]. DOI: 10.1016/S1385-8947(02)00025-6. ISSN 13858947. Dostupné z: http://linkinghub.elsevier.com/retrieve/pii/S1385894702000256

WANG, S, M SOUDI, L LI a Z ZHU. Coal ash conversion into effective adsorbents for removal of heavy metals and dyes from wastewater. Journal of Hazardous Materials [online]. 2006, 133(1-3), 243-251 [cit. 2018-06-11]. DOI: 10.1016/j.jhazmat.2005.10.034. ISSN 03043894. Dostupné z: http://linkinghub.elsevier.com/retrieve/pii/S0304389405006321

XIE, Jiting a Obada KAYALI. Effect of initial water content and curing moisture conditions on the development of fly ash-based geopolymers in heat and ambient temperature. Construction and Building Materials [online]. 2014, 67, 20-28 [cit. 2018-04-30]. DOI: 10.1016/j.conbuildmat.2013.10.047. ISSN 09500618. Dostupné z: http://linkinghub.elsevier.com/retrieve/pii/S0950061813009689

YE, Hailong a Aleksandra RADLIŃSKA. Fly ash-slag interaction during alkaline activation: Influence of activators on phase assemblage and microstructure formation. Construction and Building Materials[online]. 2016, 122, 594-606 [cit. 2018-03-14]. DOI: 10.1016/j.conbuildmat.2016.06.099. ISSN 09500618. Dostupné z: http://linkinghub.elsevier.com/retrieve/pii/S0950061816310273

YE, Hailong a Aleksandra RADLIŃSKA. Shrinkage mitigation strategies in alkali-activated slag. Cement and Concrete Research [online]. 2017, 101, 131-143 [cit. 2018-06-11]. DOI: 10.1016/j.cemconres.2017.08.025. ISSN 00088846. Dostupné z: http://linkinghub.elsevier.com/retrieve/pii/S000888461630093X

YUSUF, Moruf Olalekan, Megat Azmi MEGAT JOHARI, Zainal Arifin AHMAD a Mohammed MASLEHUDDIN. Effects of H_2O/Na_2O molar ratio on the strength of alkaline activated ground blast furnace slag-ultrafine palm oil fuel ash based concrete. Materials & Design (1980-2015) [online]. 2014, 56, 158-164 [cit. 2018-03-14]. DOI: 10.1016/j.matdes.2013.09.078. ISSN 02613069. Dostupné z: http://linkinghub.elsevier.com/retrieve/pii/S0261306913009722

ZHANG, Jin, Yan HE, Yi-pin WANG, Jin MAO a Xue-min CUI. Synthesis of a self-supporting faujasite zeolite membrane using geopolymer gel for separation of alcohol/water mixture. Materials Letters [online]. 2014, 116, 167-170 [cit. 2018-04-30]. DOI: 10.1016/j.matlet.2013.11.008. ISSN 0167577X. Dostupné z: http://linkinghub.elsevier.com/retrieve/pii/S0167577X13015255

ZHANG, Mo, Tahar EL-KORCHI, Guoping ZHANG, Jianyu LIANG a Mingjiang TAO. Synthesis factors affecting mechanical properties, microstructure, and chemical composition of red mud–fly ash based geopolymers. Fuel [online]. 2014, 134, 315-325 [cit. 2018-05-21]. DOI: 10.1016/j.fuel.2014.05.058. ISSN 00162361. Dostupné z: http://linkinghub.elsevier.com/retrieve/pii/S0016236114005201

ZHANG, Yaojun a Licai LIU. Fly ash-based geopolymer as a novel photocatalyst for degradation of dye from wastewater. Particuology [online]. 2013, 11(3), 353-358 [cit. 2018-05-21]. DOI: 10.1016/j.partic.2012.10.007. ISSN 16742001. Dostupné z: http://linkinghub.elsevier.com/retrieve/pii/S1674200113000680

ZHANG, Zuhua, Liangfeng LI, Dongning HE, Xue MA, Chunjie YAN a Hao WANG. Novel self-supporting zeolitic block with tunable porosity and crystallinity for water treatment. Materials Letters [online]. 2016, 178, 151-154 [cit. 2018-06-02]. DOI: 10.1016/j.matlet.2016.04.214. ISSN 0167577X. Dostupné z: http://linkinghub.elsevier.com/retrieve/pii/S0167577X16307194

ZHANG, Zuhua, Hao WANG, Yingcan ZHU, Andrew REID, John L. PROVIS a Frank BULLEN. Using fly ash to partially substitute metakaolin in geopolymer synthesis. Applied Clay Science [online]. 2014B, 88-89, 194-201 [cit. 2018-05-21]. DOI: 10.1016/j.clay.2013.12.025. ISSN 01691317. Dostupné z: http://linkinghub.elsevier.com/retrieve/pii/S0169131713004420

6 AUTHOR'S CURRICULUM VITAE

Personal information	
Name	**Ing. et Bc. Pavel Kejík**
E-mail	pavelkejik@vut.cz
Phone	+420 54114 4912
Date of Birth	16.12.1987
Education	
Dates	2012 - 2018
Degree	Doctoral
Discipline	Applied Sciences in Engineering
Organization	Brno University of Technology, Faculty of Mechanical Engineering
Dates	2010 - 2012
Degree	Master's
Discipline	Chemistry, Technology and Properties of Materials
Organization	Brno University of Technology, Faculty of Chemistry
Dates	2008 - 2013
Degree	Bachelor's
Discipline	Microbiology
Organization	Masaryk University, Faculty of Science
Dates	2007 - 2010
Degree	Bachelor's
Discipline	Chemistry, Technology and Properties of Materials
Organization	Brno University of Technology, Faculty of Chemistry
Selected Experience	
Dates	2010
Discipline	Materials Engineering, Winter Semestral Traineeship
Organization	Istituto Superior Técnico, Lisbon, Portugal
Dates	2013 – 2014
Discipline	Solid/Liquid Separation Internship
Organization	Lappeenranta University of Technology, Finland

ABSTRACT

A lot of applications use inorganic filtering media based on materials that use primary resources and their production is energy-intensive and thus costly and environmentally harmful. The aim of this study is to verify whether alkali-activated materials based on secondary resources, namely blast furnace slag (BFS) and fly ash (FA), can be used to produce porous media which could possibly replace ceramic and other inorganic filters.

The research question was addressed using an experimental design based on an in-house developed MATLAB calculation scheme for composition mixtures based on the most important oxide ratios in the input raw materials. This way, the greatest control of the variable composition of the inputs was ensured. In addition, the work is more relevant in general because this computational tool takes the basic oxide composition of the resources into account, so the results can be generalized. The author also designed a pure one solid component mixture series for a comparison and better characterization of the effects of composition changes on the resulting product properties.

The findings show that the strength of the 24-hour, 70 °C cured materials can exceed 7.6 MPa under a four point bending tensile test (in accordance with ČSN EN 12390-5), but to achieve a good porosity, the strength is always decreased. In the final composition slightly above 6.3 MPa was achieved. In general, the results show that the SiO_2/Al_2O_3 ratio and the amount of alkali activator affect the strength the most. Pure BFS-based mixtures show more than twice the strength of the pure FA-based samples within the given compositions used for the experiments.

The fineness of the pores achieved using fractionated raw materials (particle sizes in the range of tens to slightly over a hundred microns) is in the order of tenths to units of microns in most cases and approximately 0.2 microns in the final composition.

The total porosity of the pressed bodies is closely under 40% which compared to the unclassified resource based materials, is nearly twice that much. Pure BFS-based samples show lower total porosities than the FA-based samples, apparently due to their entirely different particle morphology – irregularly angular in BFS and round in FA.

The efflorescence phenomenon was mostly observed on FA-based materials. Energy-dispersive spectrometry (EDS) confirmed sodium hydroxide crystals undergoing gradual carbonation by atmospheric CO_2.

Permeability testing required asymmetrical barriers preparation due to the very fine porosity of the material. The asymmetrical barriers achieved water permeability of 138 $L/h.m^2$.bar and air permeability of 1320 $L/h.m^2$.bar.

ABSTRAKT

V mnoha oborech jsou stále využívána anorganická filtrační media založená na materiálech, jejichž výroba využívá primární suroviny. Jejich výroba je tedy energeticky náročná a v důsledku nákladná a neohleduplná k životnímu prostředí. Cílem této práce je ověřit možnost využití alkalicky aktivovaných materiálů na bázi sekundárních surovin, především vysokopecních strusek (BFS) a popílků z uhelných elektráren (FA), pro výrobu porézních médií schopných v budoucnosti nahradit keramické a jiné anorganické filtry.

Výzkum je rozvinut skrze experimentální design založený na výpočetním schématu samostatně vyvinutém s pomocí programu MATLAB. Toto schéma počítá vhodná složení směsí na základě poměrů obsahu nejdůležitějších oxidů ve vstupních surovinách. Tak je zajištěno zohlednění proměnlivého složení vstupních surovin a práce je tím hodnotnější, že její výsledky jsou skrze početní nástroj zohledňující základní oxidové složení surovin zobecnitelné. Zároveň byly však pro srovnání a lepší názornost závislostí vlastností na složení navrhnuty a připraveny i série vzorků založené vždy pouze na jedné ze surovin.

Z výsledků vyplývá, že pevnost vzorků z těchto směsí (vytvrzených 24 hodin při 70 °C) ve čtyřbodové ohybové zkoušce dle ČSN EN 12390-5 může přesáhnout 7,6 MPa. Dosažením co možná nejvyšší porozity však zákonitě negativně ovlivňuje pevnost materiálu a výsledný materiál tedy dosahuje pevnosti těsně nad hranicí 6,3 MPa. Výsledky obecně dokazují, že nejvíce je pevnost materiálů ovlivněna poměrem SiO_2/Al_2O_3 a množstvím alkalického aktivátoru. Z výsledků vyplývá, že alkalicky aktivované materiály (AAM) na bázi strusky dosahují i více než dvojnásobné pevnosti analogických materiálů na bázi elektrárenského popílku.

Velikost pórů materiálů připravených z tříděných surovin s velikostí zrna od desítek po lehce přes sto mikronů se ve většině případů pohybuje v rozmezí desetin ž jednotek mikronů, v případě výsledného materiálu je to pak přibližně 0,2 mikronu.

Celková porozita lisovaných těles se pohybuje těsně pod 40 %, což je v tomto případě téměř dvojnásobek ve srovnání s totožnými materiály na bázi netříděných surovin. Výsledky rovněž ukazují, že materiály na bázi strusky vykazují nižší porozitu než ty na bázi popílku, což je patrně způsobeno rozdílnou morfologií částic obou materiálů – částice strusky jsou nepravidelně hranaté a částice popílku kulaté.

V průběhu experimentální činnosti byla pozorována tvorba výkvětů u materiálů na bázi elektrárenských popílků. Pomocí Energo-disperzní spektroskopické analýzy (EDS) byly výkvěty identifikovány jako hydroxid sodný procházející karbonatací za účasti vzdušného CO_2.

Test permeability vyžadoval, kvůli velmi jemné povaze porézní struktury, přípravu asymetrických filtračních přepážek. Tyto přepážky dosáhli propustnosti 138 L/h.m^2.bar pro vodu a 1320 L/h.m^2.bar pro vzduch.